Mathematical Biosciences 378 (2024) 109337

Contents lists available at ScienceDirect

Mathematical Biosciences

journal homepage: www.elsevier.com/locate/mbs

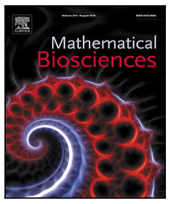

Modeling the interplay between disease spread, behaviors, and disease perception with a data-driven approach

Alessandro De Gaetano [a,b,*], Alain Barrat [a,1], Daniela Paolotti [b,1]

[a] Aix Marseille Univ, Université de Toulon, CNRS, CPT, Marseille, France
[b] ISI Foundation, Turin, Italy

ARTICLE INFO

Keywords:
Compartmental model
Disease perception
Perceived severity
Human behavior
Epidemiological dynamics
Mathematical modeling

ABSTRACT

Individuals' perceptions of disease influence their adherence to preventive measures, shaping the dynamics of disease spread. Despite extensive research on the interaction between disease spread, human behaviors, and interventions, few models have incorporated real-world behavioral data on disease perception, limiting their applicability. In this study, we propose an approach to integrate survey data on contact patterns and disease perception into a data-driven compartmental model, by hypothesizing that perceived severity is a determinant of behavioral change. We explore scenarios involving a competition between a COVID-19 wave and a vaccination campaign, where individuals' behaviors vary based on their perceived severity of the disease. Results indicate that behavioral heterogeneities influenced by perceived severity affect epidemic dynamics, in a way depending on the interplay between two contrasting effects. On the one hand, longer adherence to protective measures by groups with high perceived severity provides greater protection to vulnerable individuals, while premature relaxation of behaviors by low perceived severity groups facilitates virus spread. Differences in behavior across different population groups may impact strongly the epidemiological curves, with a transition from a scenario with two successive epidemic peaks to one with only one (higher) peak and overall more numerous severe outcomes and deaths. The specific modeling choices for how perceived severity modulates behavior parameters do not strongly impact the model's outcomes. Moreover, the study of several simplified models indicate that the observed phenomenology depends on the combination of data describing age-stratified contact patterns and of the feedback loop between disease perception and behavior, while it is robust with respect to the lack of precise information on the distribution of perceived severity in the population. Sensitivity analyses confirm the robustness of our findings, emphasizing the consistent impact of behavioral heterogeneities across various scenarios. Our study underscores the importance of integrating risk perception into infectious disease transmission models and gives hints on the type of data that further extensive data collection should target to enhance model accuracy and relevance.

1. Introduction

The propagation patterns of infectious diseases are shaped by human interactions, movements, and individual conduct. Reciprocally, the dynamic unfolding of contagious illnesses can impact human behavior [1–3]. Therefore, the interplay between disease spreading, human behaviors, and interventions, both pharmaceutical and non-pharmaceutical, has been largely studied in literature during the last twenty years (for reviews see [3–5]). Several works have integrated these different elements in various mathematical modeling frameworks, to gain quantitative insights and provide predictions and projections. Nonetheless, most of these models were limited to theoretical investigations and were not informed by representative, real-world, timely data on the behavioral aspects, largely due to the lack of availability of such data. This situation has however evolved since the emergence of SARS-CoV-2 and the resulting COVID-19 pandemic, which stimulated important data collection efforts to better inform models and gain insights into the spread of SARS-CoV-2 at various scales [6–10]. In particular, numerous studies have focused during this pandemic on evaluating the effectiveness of Non-Pharmaceutical Interventions (NPIs) and government-imposed restrictions to mitigate the contagion [11–15], as well as on assessing the benefits of vaccination campaigns [16–18].

In the current post-pandemic period, however, top-down emergency measures have been discontinued, and the responsibility for adopting

* Corresponding author at: Aix Marseille Univ, Université de Toulon, CNRS, CPT, Marseille, France.
E-mail address: alessandro.degaetano@isi.it (A. De Gaetano).
[1] A.B. and D.P. contributed equally to this work.

https://doi.org/10.1016/j.mbs.2024.109337

Available online 5 November 2024

protective measures is left to individuals. Possible protective measures encompass both aspects of each individual's social life, such as reducing social gatherings, and hygiene- or health-related practices, including mask-wearing and vaccination decisions [19]. Disease perception, i.e., the way individuals perceive how the disease might impact them, plays an important role in the adoption of such protective behaviors as evidenced by numerous studies and taken into account in psychological models (e.g. Health Belief Model) [20–22]. For instance, individuals who perceive a higher risk are more likely to adopt recommended hygiene and avoidance behaviors [23], and this relationship strengthens throughout an epidemic [24]. However, and despite the vast literature that proves its influence on behavioral aspects [23–27], risk perception has rarely been included in data-driven modeling frameworks in particular for lack of data. Consequently, the collection of data on disease perception and social contacts during the pandemic presents an interesting opportunity to investigate the impact of risk-perception-driven behaviors and behavioral changes on the propagation of a disease in a population.

In this paper, we propose to leverage data collected during the pandemic to build a partially data-driven mathematical modeling framework and investigate the complex relationship between self-adopted protective behaviors, disease spreading, and risk perception. Even if available data remains limited in scope and generalizability, they have been collected with the goal of informing models about realistic behaviors that people adopt during public health crisis. Our framework is an attempt at using such survey data when possible, still relying on several modeling choices on how disease perception may impact behavioral changes. The scenario we envision presents a competition between an ongoing wave of COVID-19 and a vaccination campaign. We however consider a context similar to the current post-pandemic period where top-down emergency measures are absent, and individuals are responsible for their protection. In this context, we develop a deterministic compartmental model that incorporates a feedback loop between behaviors, vaccines, and the contagion process and that includes risk perception as a key determinant of the adoption or relaxation of individual protective behaviors.

We build the data-driven aspect of the model using the quantitative insights into both the contact patterns of individuals and their disease perception obtained from the CoMix survey [7], in the following way. On the one hand, we model different levels of compliance with protective behaviors by two different contact matrices giving the average number of contacts between individuals of different age groups. On the other hand, we stratify the population according not only to age classes but also to how individuals perceive whether the disease poses a threat to them. Specifically, we classify individuals according to their "perceived severity", i.e., on their belief of the seriousness of the disease if they were to catch it. Perceived severity has indeed been found to be one of the most important factors impacting self-initiated behavioral changes in the context of the recent COVID-19 pandemic [23,24,28–32], including a strong association with a reduction in the number of contacts [33]. To fully define the model, we make some assumptions for the specific mathematical expression of the individual perceived severity dynamics. In particular, we hypothesize that the adoption and the relaxation of protective behaviors depend on objective indicators, given respectively by the burden of the epidemic on the hospitals and by the fraction of vaccinated individuals in the population, and can also be influenced by perceived severity. We can thus investigate within such a framework whether taking into account the population differences in perceived severity leads to differences in the epidemic dynamics and the propagation outcome in terms of various metrics such as the overall death rate and ICU peak height and date. Moreover, we consider several possible methods of informing the model's parameters by the perceived severity of individuals and explore whether they impact the model's outcome. We explore several scenarios encompassing distinct behavioral and epidemiological conditions to validate the robustness of our findings.

Results reveal that introducing differences in behavioral change parameters based on perceived severity produces differences in the timing of the epidemic curves, with an earlier peak of infections if compared to the scenario where the entirety of the population behaves in the same way. This has a crucial consequence on a model's predicted outcome as, in a progressively vaccinated population, an early peak of infections leads to a higher number of deaths. We also find that, within our framework, the precise way of modeling how the perceived severity modulates the parameters ruling the adoption and relaxation of behaviors does not strongly impact the model's phenomenology and outcome. As our modeling framework relies on data that might be difficult to collect in large populations and also subject to changes depending on the precise design of the survey (e.g., precise phrasing or ordering of the questions) [34], we consider several simpler models to investigate the impact of the various assumptions and data in the rich phenomenology exhibited by the model. We find in particular that, while information on age-stratified contact patterns plays an important role, it is possible to rely on imprecise data when building the distributions of perceived severity and describing their interplay with age groups.

These results have direct public health implications: on the one hand, they highlight a certain robustness with respect to some unavoidable arbitrariness in modeling choices and with respect to fluctuations in the data on disease perception. On the other hand, they emphasize the need to gather more extensive data on how the perception of risks correlates with behavioral change in various populations and possibly different epidemiological contexts, to build data-informed models taking into account risk perception.

2. Materials and methods

2.1. Data

We leverage data collected during the pandemic period, namely through the CoMix survey [7,33] initiative, to (i) generate age-stratified contact matrices corresponding to different levels of compliance with respect to self-adopted protective measures and (ii) additionally stratify the population according to the perception of individuals of the risk posed by the disease. The CoMix study developed a longitudinal survey approach for the collection of data aiming at a better comprehension of the behaviors of individuals throughout the COVID-19 pandemic. The surveys, administered every two weeks, captured the evolving awareness, attitudes, and behaviors of participants in response to COVID-19, together with comprehensive information on age, gender, occupation, physical contacts, COVID-19 testing, and self-isolation. It was launched initially in March 2020 in Belgium, the Netherlands, and the United Kingdom, and further expanded its reach to an additional 17 European countries.

We focused our study on the case of Italy where, during the winter between 2020 and 2021, the government implemented a tiered regional system of restrictive measures, with progressively stricter tiers — yellow, orange, and red zones [35]. We use the contact patterns measured in the red zones as a proxy for contacts among individuals adopting highly restrictive protective measures, while contact matrices measured among individuals living in areas where the yellow zone restrictions were implemented represent a situation where individuals adopted less restrictive measures and have a higher number of contacts with respect to what happens in the red zones. We first stratify the population into seven age groups (0–4, 5–17, 18–29, 30–39, 40–49, 50–59, and 60+), using data about the population distribution in Italy across the various age groups from the 2019 United Nations World Population Prospects [36]. We then use the data from the CoMix survey for Italy to generate two contact matrices: the one resulting from data collected in the red zone is used in the model to reflect the contacts of individuals who adopt protective behaviors (named in the rest of the paper as "compliant" individuals), while we use the one built from

the yellow zone data to describe the contacts of what we call "non-compliant" individuals (see [37] for more detailed information on the specific top-down restrictions imposed by health authorities during the data collection).

In addition to questions related to their contacts (e.g. total number, frequency, location, etc. — see [37] for detailed information on the contact surveys), participants over 18 years old answered questions related to their risk perception. Concerning perceived severity, participants were asked to indicate their agreement with the statement "Coronavirus would be a serious illness for me" using a 5-point Likert scale ranging from strongly disagree to strongly agree. This information allowed us to further stratify the population in each age group into 5 specific perceived severity subgroups based on participants' responses (denoted by 1 for low perceived severity, i.e. for the "strongly disagree" answer to 5 for the "strongly agree" denoting a high perceived severity) [7,33]. For individuals who have participated in more than one wave of data collection, we averaged the scores of their perceived severity responses across waves and we assigned them to the closest of the 5 groups. In this way, we assumed that the perceived severity of individuals remains the same over time. For individuals under 18, given the absence of direct data on perceived severity, we assumed that their perceptions were predominantly shaped by their parents. Thus, we categorized age groups 0–4 and 5–17 into subgroups based on the perceived severity responses provided by individuals of parental age (20 to 50 years old). This decision is supported by [38], in which an analysis conducted on adolescents between 13 and 20 years old in Italy during the lockdown evidenced a distribution of perceived severity among them similar to the one we obtained aggregating the data of individuals aged 20 to 50.

Having stratified individuals within each of the 7 age groups into 5 perceived severity groups, we obtain an overall population divided into 35 subgroups. While the survey data gives, for each reported contact, the age groups of both the reporting participant and the individual with whom the contact took place, this is not the case for the perceived severity (only the one of the reporting participant is known). We thus assume that, for a contact with an individual in a given age group i, the probability that this individual has a certain perceived severity p is simply given by the fraction N_{ip}/N_i of such individuals in their age group i (where N_g indicates the number of individuals in group g). We thus build 35×35 contact matrices by multiplying each element of the age-stratified contact matrices by the fraction of the population in each perceived severity group. To this aim, we first consider the total number of contacts $c_{ii'}$ between individuals in age group i and age group i' and define $m_{ipi'p'}$ as the total number of contacts of individuals in age group i and perceived severity p with individuals in age group i' and perceived severity group p'. Both these matrices are symmetrical and, given the above assumption, we have:

$$m_{ipi'p'} = c_{ii'} * \frac{N_{ip}}{N_i} * \frac{N_{i'p'}}{N_{i'}} .$$

To feed the model, we need, instead of m, the contact matrix which gives the number of contacts per person in the age group i and perceived severity group p with individuals of age group i' and perceived severity p', i.e., $M_{ipi'p'} = \frac{m_{ipi'p'}}{N_{ip}}$. By substituting and using the analogous formula linking the age-stratified contact matrix C with the numbers of contacts between age groups c, i.e., $C_{ii'} = \frac{c_{ii'}}{N_i}$, we obtain:

$$M_{ipi'p'} = C_{ii'} * \frac{N_{i'p'}}{N_{i'}} . \quad (1)$$

Note that M, just as the usual contact matrix C, is not symmetrical as it gives a number of contacts per participant. Due to the hypothesis made in its construction, it also depends linearly on the number of individuals in the perceived severity group p' and age group i', but not on the perceived severity of the contacting individual.

We finally note that the CoMix survey participants also expressed their perceived susceptibility and risk with the following two statements: "I am likely to catch coronavirus" and "I am worried that I might spread coronavirus to someone who is vulnerable". However, we did not include these variables in the analysis because their association with the number of contacts, in the context of the COVID-19 emergency, was found to be less relevant in [33].

2.2. Model definition

We consider a deterministic compartmental model similar to the one used in [17], to describe the propagation of SARS-CoV-2 in a population stratified by age and perceived severity of the disease (7 age classes and 5 perceived severity classes). The model incorporates on the one hand a vaccination process and on the other hand a behavioral component. The latter describes the possibility of modifying one's contact patterns depending on the unfolding of the epidemic and it is modulated by a data-informed perceived severity attribute. Fig. 1 presents a diagrammatic sketch of the model, which we now describe in detail. A more in-depth explanation of the scenario explored and the sources of the parameters are reported in Section 2.3. We moreover report in the Supplementary Material the full set of evolution equations describing the model.

2.2.1. Compartmental model

Each individual can transition from one compartment to the other depending on their status with respect to the disease, their vaccination status, and their current behavior.

Susceptible individuals (S compartment) in contact with infectious individuals can be infected and transition into the latent (L compartment). They then enter the pre-symptomatic (P) stage of the infection with a constant rate ϵ. They leave the pre-symptomatic stage at a constant rate ω, reaching either the asymptomatic compartment A with age-dependent probability f, or the symptomatic infectious compartment I (with probability $1-f$). Asymptomatic individuals recover at rate μ, entering the recovered compartment R. Symptomatic infectious individuals can either recover, be hospitalized in the Intensive Care Unit (ICU compartment), or die (D compartment), with rate μ in all cases. The respective probabilities are determined, as described in detail in the Supplementary Material, by the three following age-stratified parameters: the Infection ICU Ratio ($IICUR$) the Infection Fatality Rate (IFR), and the Probability of deaths among ICU ($PICUD$). Finally, individuals leave the ICU compartment at rate $1/\Delta$, where Δ represents the mean number of days of hospitalization. They then either die with probability $PICUD$ or recover with probability $1-PICUD$.

The force of infection resulting from contacts between susceptible and symptomatic infectious individuals (compartment I) is determined by an age- and perceived severity-stratified "compliant" contact matrix (corresponding to Italy's red zones) M^C, whose elements $M^C_{iji'j'}$ represent the average number of contacts that an individual in age group i and perceived severity group j has with individuals in age group i' and perceived severity group j' per day, and multiplied by a transmission rate β. The transmission rate from pre-symptomatic and asymptomatic individuals is reduced by a factor $\chi < 1$.

We moreover model a vaccination process as follows: each day, a fraction of the susceptible population receives a vaccine and transitions to the V compartment. The rollout rate r_V represents the number of daily available doses expressed as a percentage of the total population. As in previous works [39,40], we assume the vaccine can reduce susceptibility with efficacy VE_S, the probability of developing symptoms with efficacy VE_{Symp}, and severe symptoms leading to death with efficacy VE_D. In practice in the model, this means that the infection rate for individuals in the V compartment is reduced by a factor $(1-VE_S)$, the probability $1-f$ of becoming infected I instead of asymptomatic A is reduced by a factor $(1-VE_{Symp})$, and the probability of transitioning from I^V to the ICU compartment and the IFR are both reduced by a factor $(1-VE_D)$. The overall efficacy of the vaccine is expressed by the following formula $VE = 1-(1-VE_S)(1-VE_{Symp})(1-VE_D)$.

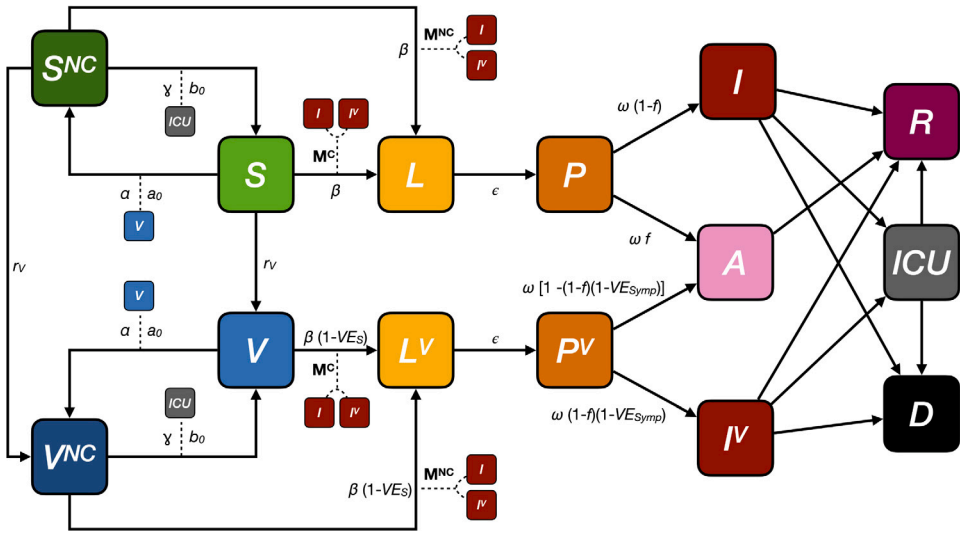

Fig. 1. Model diagram. The model is an extension of a standard SLIR (Susceptible-Latent-Infected-Recovered) with the addition of individuals who are pre-symptomatic (P) and asymptomatic (A) and also individuals in Intensive Care Units (ICU), and individuals who die (D). Furthermore, we introduced an additional series of compartments for vaccinated individuals (V, L^V, P^V, I^V) and two compartments (S^{NC} and V^{NC}) for individuals that relax their protective behaviors. Those individuals have a higher risk of infection, modeled using a contact matrix M^{NC} with a greater number of contacts than the one used for compliant compartments (S and V), M^C. Both matrices M^C and M^{NC} capture contact patterns of the winter period 2020–2021 in Italy, for regions with, respectively, high and small stringent restrictions.

2.2.2. Coupling disease dynamics, behavior and vaccination

We assume that individuals, during the epidemic, can change behavior. Specifically, there is a possibility that individuals, both susceptible (S) and vaccinated (V), may abandon safe behaviors and expose themselves to higher risks of infection. To incorporate this behavioral change, we introduce two additional compartments, S^{NC} and V^{NC}, where NC stands for non-compliant individuals. We thus assume that these non-compliant individuals have contacts described by Italy's yellow zone contact matrix M^{NC} (thus with more contacts than for the S and V compartments and consequently a higher probability of being infected). For the convenience of notation, we will hereafter denote by C the union of the compliant compartments S and V, and by NC the non-compliant compartments S^{NC} and V^{NC}.

Our model's crucial hypothesis concerns the interplay between behavioral change, vaccination, and the unfolding of the disease spread, which determines the transitions between compliant and non-compliant compartments. We first assume that the transition rate from C to NC, $\lambda_{X->X^{NC}}$ ($X = S$ or $= V$) describing the relaxation of protective behavior, increases with the fraction of vaccinated people v_t in the population. This expresses the idea that individuals may consider that the threat posed by the disease is lower if more people are vaccinated. Second, we assume on the other hand that the transition rate from NC to C, $\lambda_{X^{NC}->X}$ ($X = S$ or $= V$), depends on the occupancy of beds in intensive care ICU_t, taken as a quantitative indicator of the overall seriousness of the spread. Finally, to incorporate all the aforementioned variables, we model both transition rates using logistic functions, described each by two parameters: a slope (α for the C to NC transition and γ for the NC to C one) and a midpoint (a_0 for the C to NC transition and b_0 for the NC to C one). The expressions of these rates are as follows (for $X = S$ and $X = V$):

$$\begin{aligned}\lambda_{X->X^{NC}} &= \frac{1}{1+\exp^{-\alpha(v_t-a_0)}}\\ \lambda_{X^{NC}->X} &= \frac{1}{1+\exp^{-\gamma\left(\frac{ICU_t}{ICU_{max}}-b_0\right)}}\end{aligned} \tag{2}$$

The choice of the logistic function is supported by several studies across different fields, which show that social contagion and the adoption of new behaviors, technologies, or social learning processes is well described by an S-shape curve [41–43]. Furthermore, compared to other accelerating diffusion curves (such as the exponential), the logistic function offers several theoretical advantages. Firstly, the presence of two parameters instead of one allows for better control over the shape of the transition. Secondly, the two parameters are easier to interpret. Thirdly, the logistic functions give non-zero rates of transitions between the compliant and non-compliant compartments even at the beginning of the simulations before the start of the vaccination campaign, so that a fraction of non compliant individuals is included from the start in a more realistic way. Fig. 2 shows the functional dependence of $\lambda_{X->X^{NC}}$ with the fraction of vaccinated individuals and illustrates how the functional shape depends on the slope α and the midpoint a_0. Similar plots and considerations stand for the rate $\lambda_{X^{NC}->X}$ as γ and b_0 vary. The way these parameters alter the transition's shape makes them suitable for variation across different population groups, enabling the introduction of behavioral differences, as we will discuss next.

2.2.3. Modulating behavioral change by risk perception

The final element of our model is the introduction of disease perception as a determinant of behavioral change. In particular, as shown in literature [33,44,45], individuals with high perceived severity have a smaller number of contacts, which in our framework corresponds to compliant behavior. For this reason, we assume that the midpoints a_0 and b_0 of the logistic functions of Eq. (2), giving the transition rates between compliant and non-compliant compartments, depend on the perceived severity. We instead fix for simplicity the values of the slopes α and γ.

As individuals with higher perceived severity should be more reluctant to relax their behavior and/or more prone to adopt protective measures (with thus fewer contacts), we assume that the midpoint a_0 is an increasing function of perceived severity ($= 1, \ldots, 5$), while b_0 is instead a decreasing function. How a_0 and b_0 precisely depend on the perceived severity represents however an a priori arbitrary modeling choice. Here we explore several possible choices for these variables, to explore the impacts different regimes might have on the overall unfolding of the epidemic. We thus consider five possible different functional forms for the relationship between midpoints and perceived severity, sketched in Fig. 3 (note that we assume for simplicity that the midpoints do not depend directly on the age group, but only through possible correlations between age and perceived severity). By going from perceived severity 1 to perceived severity 5, these functions all have a part displaying a linear growth, and either one or two flat parts, i.e., groups with neighboring values of perceived severity sharing the same midpoint value. For simplicity, in the remainder of the study

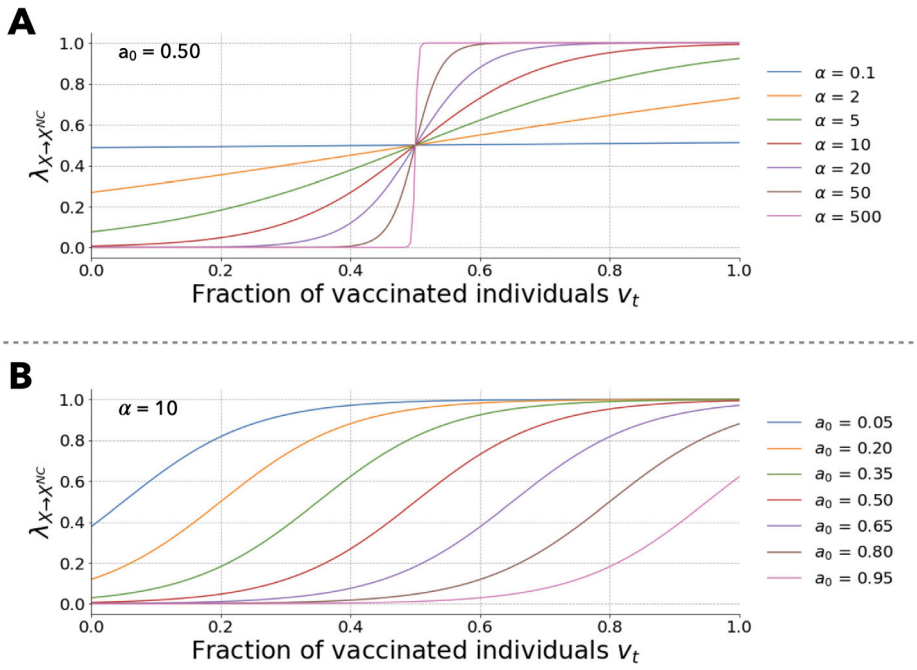

Fig. 2. Rate of transition from compliant to non-compliant compartments as a function of the fraction of vaccinated population for several values of (A) the slope α with a fixed midpoint of $a_0 = 0.5$, and (B) the midpoint a_0 with a fixed slope of $\alpha = 10$.

we denote those functions by the following names, which describe the location of the linear growth part: Growth, Center Growth, Start End Growth, Start Growth, and End Growth. Naming a_{0_j} the value of a_0 for the perceived severity group j ($j = 1$ to 5), we have:

- Growth: linear growth of the midpoint for all five perceived severity groups $a_{0_j} = mj + q$
- Central Growth: linear growth for the three central perceived severity groups and the same value of the parameters for the two lowest perceived severity groups and for the two highest $a_{0_j} = mj + q$ for i=2, 3, 4, with $a_{0_1} = a_{0_2}$ and $a_{0_4} = a_{0_5}$.
- Start End Growth: linear growth for the two lowest perceived severity groups and for the two highest and the same value of the parameters for the three central perceived severity groups $a_{0_j} = mj + q$ for $i = 1$, 2 and for $i = 4,5$, with $a_{0_2} = a_{0_3} = a_{0_4}$.
- Start Growth: linear growth for the three lowest perceived severity groups and the same value of the parameters for the others $a_{0_j} = mj + q$ for $i = 1,2,3$, with $a_{0_3} = a_{0_4} = a_{0_5}$.
- End Growth: linear growth for the three highest perceived severity groups and the same value of the parameters for the others $a_{0_j} = mj + q$ for $i = 3,4,5$, with $a_{0_1} = a_{0_2} = a_{0_3}$.

In all cases, the average of the individual midpoints in the population is given by $\overline{a_0} = \frac{\sum_{i=1}^{5} n_i a_{0_i}}{\sum_{i=1}^{5} n_i}$, where each value a_{0_i} of the midpoint is weighted by the population having that value, i.e., by the population n_i of individuals with perceived severity i. If behaviors are not dependent on perceived severity (flat functions, $m = 0$), then the midpoint takes the value $\overline{a_0}$ for all groups. Else, different groups can have different midpoints. A natural way to quantify the corresponding variation among groups is then given by the weighted variance of the midpoints, $\sigma^2_{a_0} = \frac{\sum_{i=1}^{5} n_i (a_{0_i} - \overline{a_0})^2}{\sum_{i=1}^{5} n_i}$, where again each deviation from the average is weighted by the size (population) of the corresponding group. We show in the Supplementary material how to express the slope m and the intercept q of each function as a function of the weighted mean $\overline{a_0}$ and of the weighted variance $\sigma^2_{a_0}$ of the midpoints. Similar calculations apply for the parameter b_0 with the only difference that the midpoint decreases with perceived severity and, thus, the slopes m take negative values. Hence, the equivalent functions used for b_0 are denoted as: Decrease, Center Decrease, Start End Decrease, Start Decrease, and End Decrease. Note that the parameters are independent of age and we consider that each individual keeps the same perceived severity over time. In this way, by fixing the mean value of the midpoint ($\overline{a_0}$ or $\overline{b_0}$) and by changing the variance ($\sigma^2_{a_0}$ or $\sigma^2_{b_0}$), we can model how differences in perceived severity lead to differences in behavioral changes, as determined by the transition rates between compliant and non-compliant compartments. Fig. 3 gives a concrete example of this framework. With a fixed mean value of the midpoint $\overline{a_0}$, if the variance $\sigma^2_{a_0}$ is equal to 0, every perceived severity group has the same midpoint, independently from the function used (dashed line). However, if we increase the variance (i.e. $\sigma^2_{a_0} = 0.05$ in the figure), different perceived severity groups have different midpoints, leading to different transition rates at a fixed fraction of vaccinated people. Moreover, these transition rates depend on the specific function considered in the model. Note that some values of the midpoints can be negative or larger than 1, resulting in the population in that group being almost entirely non-compliant or compliant for the whole simulation, as their transition rate to the non-compliant compartment is then either always very high or always very small.

Fig. 3 focuses on the transition from the compliant to the non-compliant compartments, but similar sketches can be drawn for the dependence of b_0 with perceived severity, albeit with decreasing shapes. We will focus in the main text on the impact of dependence of a_0 on the perceived severity, varying the mean value of the midpoint $\overline{a_0}$ and the variance $\sigma^2_{a_0}$, at fixed values of the slopes $\alpha = 10$ and $\gamma = 5$, and considering the case of $\overline{b_0} = 0.75$ with $\sigma^2_{b_0} = 0$ (i.e., no dependence on perceived severity for the transition rate to the compliant compartments). In the Supplementary Material, we perform a sensitivity analysis by varying α, γ, and $\overline{b_0}$, and consider as well the case of b_0 depending on the perceived severity.

Finally, in our framework, perceived severity only affects how people behave. Indeed, the perceived severity of a disease by an individual is not linked to the actual severity if the individual becomes infected, so severe outcomes do not depend on perceived severity. However, there may be a spurious correlation, with frail individuals perceiving higher

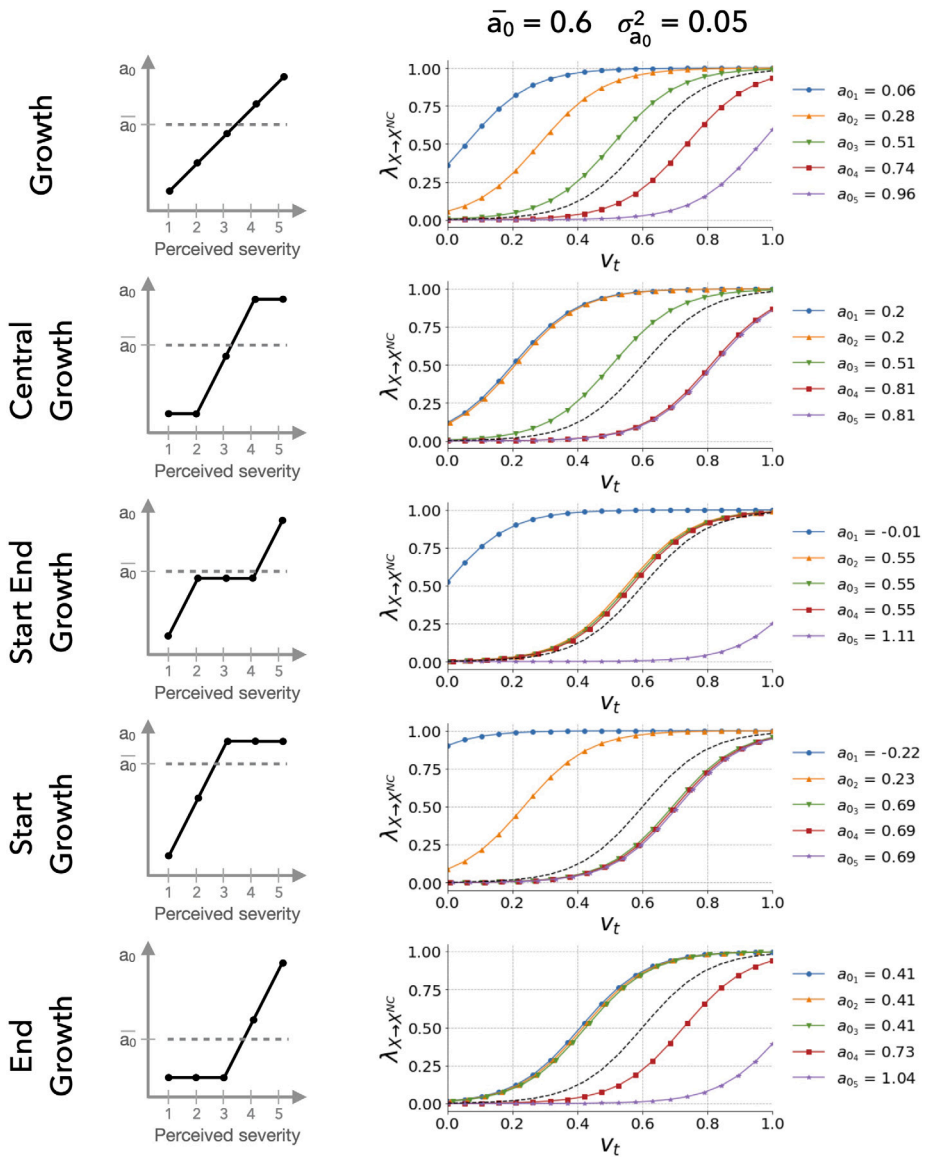

Fig. 3. Left column: Sketch of the 5 functions used to model the dependency of the midpoint from perceived severity. From top to bottom, Growth, Central Growth, Start End Growth, Start Growth, End Growth. The horizontal dashed lines give the average $\overline{a_0} = 0.6$. Right column: logistic curves as a function of the fraction of vaccinated individuals, for the various midpoints obtained with a fixed average $\overline{a_0} = 0.6$ and either variance 0 (dashed line, in which case all midpoints are equal to the average) or variance $\sigma^2_{a_0} = 0.05$.

severity and having a higher risk of severe outcomes; this is partly accounted for by associating severe outcomes with age, where elderly individuals generally have a higher perceived severity.

2.3. Model parameters and scenario

Epidemiological parameters. We consider a scenario inspired by the one unfolding in Italy starting in mid-2021, as this corresponded to the deployment of the vaccination campaign against SARS-CoV-2. We therefore use epidemiological parameters matching the characteristics of the Delta variant, which was the dominant one in Italy at that time. In particular, the parameters ϵ, ω and μ are taken from the literature [46–50].

The fraction of asymptomatic individuals is age-dependent and taken from [51], where we grouped the asymptomatic and pauci-symptomatic individuals, given that the latter show no clear signs allowing us to identify their disease. Individuals in pre-symptomatic and asymptomatic compartments have lower infectiousness (with respect to the symptomatic ones), quantified by the parameter χ, which we take from [52], in line with the value used in other models such as [17,53].

We tune β to obtain a value of R_0 between 1 and 2.5 in all cases. Indeed, even if the value of R_0 for COVID-19 has reached larger values during the pandemic, in particular during the first wave of 2020 [51,54,55], we limited our investigation to such values to include the impact of the restrictions adopted to mitigate the spread directly into R_0 in an effective way.

We provide in the Supplementary material the detailed computation of the formula yielding the model's basic reproduction number R_0, which we report here for convenience:

$$R_0 = \beta \left(\frac{\chi}{\omega} + \frac{1-f}{\mu} + \frac{\chi f}{\mu} \right) \rho(\widetilde{M}^C + \widetilde{M}^{NC}) \,, \tag{3}$$

where ρ is the spectral radius and $\widetilde{M}^C_{ii'jj'} = \frac{\phi_j}{1+\phi_j} \frac{N_{ij}}{N_{i'j'}} M^C_{ii'jj'}$ and $\widetilde{M}^{NC}_{ii'jj'} = \frac{1}{1+\phi_j} \frac{N_{ij}}{N_{i'j'}} M^{NC}_{ii'jj'}$ are the two contact matrices weighted by the relative population in different age and perceived severity groups. These matrices also take into account that the initial fraction of compliant

Table 1
Parameters of the model, with their corresponding values and sources of the literature.

Parameters	Symbols	Value	Source
Epidemiological			
Transmission rate	β	0.08	[51,54,55]
Inverse of the latent period	ϵ	0.25 days^{-1}	[46–48]
Inverse of the presymptomatic period	ω	0.56 days^{-1}	[46] [47,48]
Inverse of recovery period	μ	0.2 days^{-1}	[49,50]
Mean occupancy of ICU bed	Δ	15 days	[56]
Reduced infectiousness of P and A	χ	0.55	[52]
Fraction of asymptomatic individuals	f	age-stratified	[51]
Reproductive number	R_0	Computed from β and μ	/
Infection fatality ratio	IFR	age-stratified	[57]
Infection ICU ratio	IICUR	age-stratified	[58]
Probability of death among ICU	PICUD	age-stratified	[59]
Available number of ICU beds	ICU_{max}	7,200	[60]
Initial number of individuals distributed in the infected compartments	i_0	550,000	[61,62]
Initial number of individuals in ICU compartments	icu_0	2,500	[61,62]
Initial fraction of people in R and D compartments	r_0, d_0	0.1, 0	[61,63,64]
Vaccination			
Rate of vaccination	r_V	0.025	[61]
Vaccination strategy	/	Reverse order of age	[39,65,66]
Vaccine efficacy against infection	VE_S	0.7	[67–69]
Vaccine efficacy against symptoms	VE_{Symp}	0.5	[67–69]
Vaccine efficacy against severe outcomes	VE_D	0.4	[67–69]
Behavioral			
Slope of logistic rate $C \to NC$	α	10	[70]
Slope of logistic rate $NC \to C$	γ	5	[70]
Midpoint of logistic rate $C \to NC$	a_0	Variable Perceived severity stratified	/
Midpoint of logistic rate $NC \to C$	b_0	Variable Perceived severity stratified	/

individuals at the simulation's outset, denoted by the term ϕ_j, is not necessarily 1.

While ϵ, ω, μ, and χ are fixed, the fraction of asymptomatic individuals f depends on age and we obtain a different value of R_0 for each age group. Moreover, the term ϕ_j depends on the behavioral parameters (α, γ, $\overline{a_0}$, $\overline{b_0}$, $\sigma^2_{a_0}$, and $\sigma^2_{b_0}$), which thus also impact the value of R_0. We refer to the Supplementary Material for more details.

We estimate for the average hospitalization period in ICU Δ a value of 15 days, based on data from the Centers for Disease Control and Prevention [56]. Indeed, for COVID-19 deaths, there was an average interval of approximately two to three weeks between the onset of symptoms and the occurrence of death.

The Infection Fatality Rate (IFR) is age-dependent and we used the values reported in [57]. The Infection ICU Ratio ($IICUR$) is obtained from [58] by multiplying the probability of hospitalization if infected and the probability of ICU if hospitalized, which are reported for each age group. On the other hand, for the Probability of Deaths among ICU ($PICUD$), which is also age-stratified, we used data from [59]. Finally, the maximum number of beds in ICU changed notably during the early phase of the pandemic in Italy, going from an initial value of around 5000 to over 8000 in the Spring of 2021. We chose to use 7200, an estimate of the number of beds in intensive care in Italy at the end of 2020 [60].

The parameter values and the corresponding literature sources are reported in Table 1.

Initial conditions. We consider a scenario in which the vaccination campaign starts as the virus has already been able to spread among the population. In the COVID-19 pandemic indeed, the beginning of the spread can be set approximately in February 2020 but the vaccines became available at the end of December 2020. This is also in line with any scenario of a newly emerging virus for which vaccines are not immediately available. We thus do not initialize the model with all individuals in the S compartment, but instead, we distribute a fraction of the population in the various infected and recovered compartments, based on observations from various sources [61–64].

We first distribute 550,000 individuals, i.e., the estimated number of active cases on the first days of 2021 in Italy [62], in the infectious compartments, namely L, P, I, and A. The repartition in these compartments is based on the average period of permanence in each compartment (ϵ^{-1}, ω^{-1} and μ^{-1}, respectively) and on the fraction of asymptomatic individuals f. The resulting number of individuals in the I compartment is 143,000, which is a middle ground between the weekly number of confirmed cases in the last weeks of 2020 (approximately 100,000) and the biweekly one (approximately 200,000) [61]. We also take into account that the ICU occupancy in Italy at the beginning of 2021 was around 2500 individuals [61]. For the initial fraction of recovered individuals we use 0.1, which corresponds to the seroprevalence obtained in independent studies in two different regions of Italy at the end of 2020 [63,64]. Finally, even if the first wave of 2020 had already caused a considerable number of victims, we set the initial number of individuals in the death compartment to 0, as we focus here only on the number of deaths during the wave we are simulating.

Vaccination. For the vaccination campaign, we used a vaccination strategy in reverse order of age which is the most effective in reducing fatalities according to the literature and was the most widely used around the world [39,65,66]. We consider a vaccination daily rate of 0.25% of the total population, similar to the rate of vaccination in Italy in Spring 2021 [61]. Finally, consistently with the estimated efficacy of vaccines against COVID-19, we used a vaccine efficacy against infection of $VE_S = 70\%$, and we selected VE_{Symp} and VE_D to achieve a global vaccine efficacy around 90% [39,65,66]. In the Supplementary Material, we also considered scenarios with a lower vaccine efficacy.

Behavioral parameters. The behavioral parameters are the ones least constrained by the available data and literature. As explained above, we considered logistic functions to describe the dependency of the transition rates between compliant and non-compliant compartments on the fraction of vaccinated individuals and on the occupancy of ICU beds. We considered five different functions for the dependency of their midpoints a_0 and b_0 on the perceived severity. We fixed the slopes of the logistic functions to $\alpha = 10$ and $\gamma = 5$. Indeed, we hypothesize that the evolution of behaviors should not have brutal threshold effects: for instance, the relaxation of behaviors during the vaccination campaign has been progressive and not triggered by a particular event [70]. The slopes we consider correspond to logistic functions that are neither too steep nor with too little variation, making them well suited to model the progressive relaxation of behaviors or their re-adoption. In the Supplementary Material, we explored the robustness of our results using other values corresponding to steeper or smoother logistic curves.

Equations and coding. We report in the Supplementary Material the full set of equations describing the evolution of the populations in the various compartments. We integrate these equations numerically with a temporal resolution of 1 day, using the odeint function of the numpy library of Python. The function uses an adaptive step size method based on the LSODA algorithm from the FORTRAN library odepack. The algorithm implements Adams and Backward Differentiation Formula methods to integrate. The rest of the analysis is conducted in Python with the libraries scipy, numpy, numba, and matplotlib for the visualization part. The code used for the analysis is available on Github [71].

3. Results

3.1. Perceived severity classes and age classes

Fig. 4 shows the distribution of the population according to age in each perceived severity group (the distribution of perceived severity in each age group is instead shown in the Supplementary Material). The numbers in the figure refer to the Italian population and they are extrapolated from the 1606 individuals who took part in the survey and who reported their perceived severity. The lowest perceived severity group is the least populated and displays a relatively even distribution across age groups. Groups of individuals with perceived severity 2 and 5 have similar sizes, and groups of perceived severity 3 and 4 are the most populated. As perceived severity increases, the relative contribution of the youngest age groups tends to decrease, and the contribution of the elderly increases. In particular, about 40% and 50% respectively of the population of the two highest perceived severity groups (4 and 5) are above 60 years old. Overall, the majority of the elderly population is in these two groups of high perceived severity (see also Supplementary Material).

In Fig. 5A, we show the distribution of perceived severity across the seven waves of data collection. The profiles are qualitatively similar, with the distributions not significantly different for the last five waves (Kolmogorov–Smirnov test p-value > 0.05).

Of the 1606 participants who reported their perceived severity, 1477 took part in more than one wave of data collection, allowing for an exploration of changes in perceived severity over time. Fig. 5B illustrates the maximum change in perceived severity. For instance, if an individual participated in five waves of data collection and reported perceived severity values between 1 and 3 in these waves, their maximum change in perceived severity would be 2. Nearly one-third of participants never changed their reported values of perceived severity, while over 40% experienced a change of just one unit. Overall, fewer than 25% of participants reported a change in perceived severity of more than two units.

In Fig. 5C, we explore the phenomenon in more depths by examining the maximum change based on the number of waves participants attended. Each bar represents the number of waves attended, with colors indicating the maximum change in perceived severity. Among participants who attended only two waves of data collection, over 50% did not change their perceived severity, and more than 85% experienced a change of no more than one unit. As the number of waves attended increases, the percentage of participants who did not change their perceived severity decreases to 22%, suggesting that over a longer time period, individuals are more likely to alter their perceived severity. However, less than one third of participants took part at six or seven waves and given that only around 30% of them changed perceived severity by more than one value, data availability becomes a limiting factor in understanding the evolution of perceived severity over time.

Given these results, we decided to maintain the hypothesis of constant perceived severity for individuals in the model, as an approximation, given that over 75% of participants experienced a maximum change of one unit, with this percentage exceeding two-thirds even among those who participated in every wave of data collection.

3.2. Basic reproduction number

The basic reproduction number R_0 depends on the age groups and on the behavioral parameters (α, γ, $\overline{a_0}$, $\overline{b_0}$, $\sigma^2_{a_0}$, and $\sigma^2_{b_0}$), as explained in Section 2.3.

Fig. 6 shows the value of R_0 as a function of $\overline{a_0}$ and $\sigma^2_{a_0}$, for three of the seven age groups and for the 5 different functions (see the Supplementary Material for the same figure including all age groups). All age groups present similar heatmaps, but younger ones present smaller reproduction numbers at equal $\overline{a_0}$ and $\sigma^2_{a_0}$ than older groups. This is mainly because the fraction of asymptomatic individuals f is much higher in the young population and asymptomatic individuals have a lower infectiousness given by parameter χ.

We first observe that R_0 decreases systematically as the average midpoint $\overline{a_0}$ value increases. Indeed, increasing $\overline{a_0}$ implies that the transition rates from compliant to non-compliant compartments decrease. As a result, even in the initial population, the fraction of non-compliant individuals (who have more contacts) decreases, leading to a reduction in R_0.

Increasing the variance $\sigma^2_{a_0}$ between the midpoints of different perceived severity groups at given $\overline{a_0}$ has a more contrasted outcome. It indeed introduces differences in the transition rates $\lambda_{X->X^{NC}}$ of different perceived severity groups, and thus the fractions of compliant individuals differ across these groups. As a result, groups of individuals with smaller perceived severity exhibit an initial higher fraction of non-compliance than groups with higher perceived severity. For small $\overline{a_0}$, the fact that groups of high perceived severity have a decreasing fraction of non-compliant individuals as $\sigma^2_{a_0}$ increases leads to a decrease in R_0. For large $\overline{a_0}$ instead, the impact on R_0 comes from the groups of small perceived severity, within which the fraction of non-compliant individuals increases and yields an increase in R_0.

The five functions yield qualitatively similar results, with some quantitative differences due to their shapes and the different distribution of young and elderly individuals in perceived severity groups. For instance, the R_0 for the function Start End Growth almost does not evolve with increased variance. This is because the three groups of intermediate perceived severity (2, 3, 4), who together represent the vast majority of the population, have the same midpoint that has only a small variation with $\sigma^2_{a_0}$. For the Start Growth function instead, R_0 drops substantially when the variance increases for small $\overline{a_0}$, because the groups with the highest perceived severity, which also contain a large fraction of elderly, have an increasing midpoint and thus an increasing fraction of compliant individuals. Conversely, for the function End Growth R_0 also decreases but remains high for small $\overline{a_0}$ as a large fraction of the population keeps a low value of the midpoint.

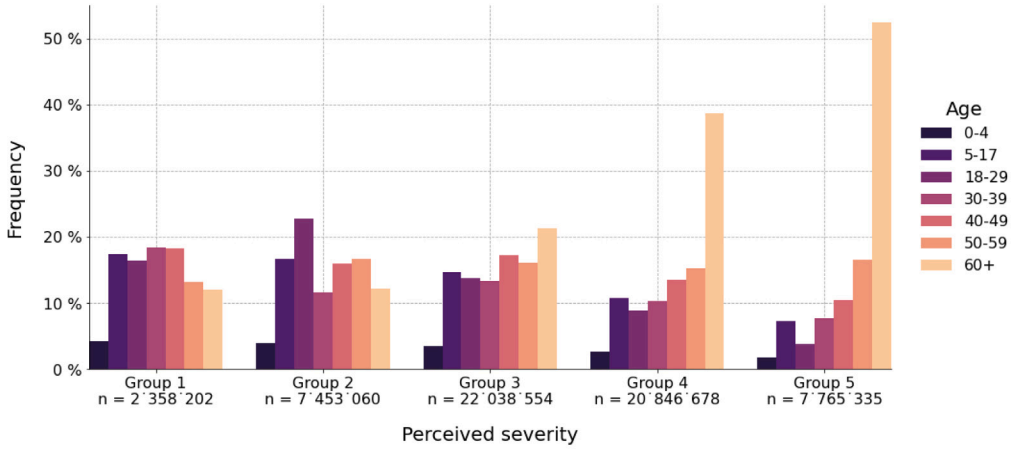

Fig. 4. Distribution of age in each perceived severity group. We also report the total number of individuals in each group.

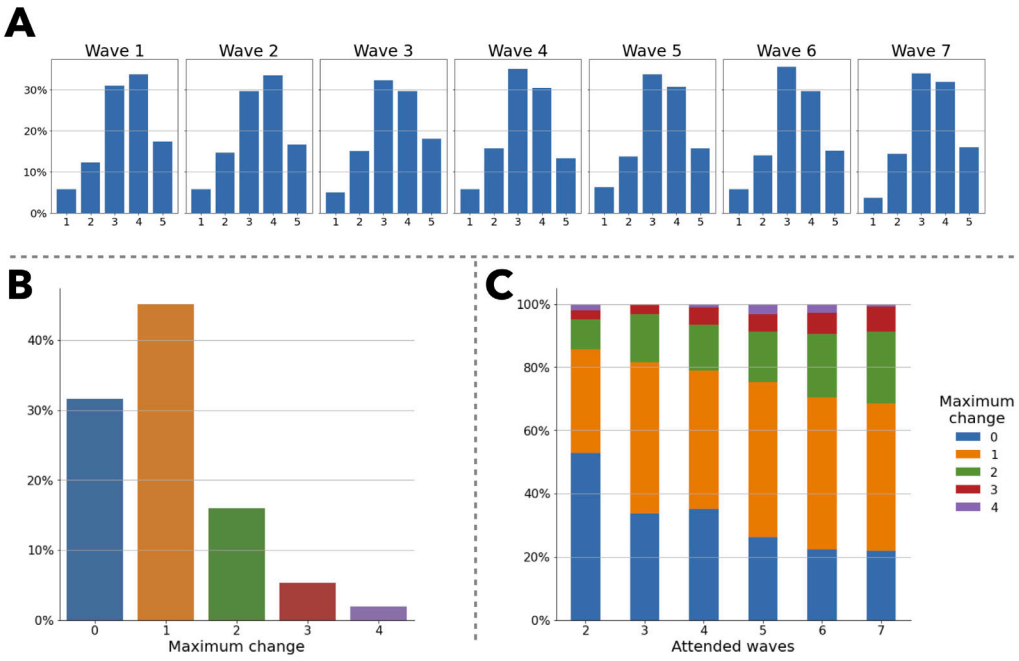

Fig. 5. Panel showing: (A) the distribution of participants in the five perceived severity groups across the seven waves of data collections, (B) the maximum change of perceived severity among individuals who took part in more than one wave, and (C) the maximum change of perceived severity over the waves of data collections disaggregated by wave. Each bar refers to the number of waves attended and it is divided in colors based on the maximum change of perceived severity. The number of participants who took part in 2 waves is 201, in 3 waves is 189, in 4 waves is 298, in 5 waves is 377, in 6 waves is 298, and in 7 waves is 114.

3.3. Effects of the heterogeneity in perceived severity on the epidemic outcome

We now turn to the impact of how perceived severity drives different types of behaviors on several metrics describing the outcome of the epidemic spread. Specifically, we measure as outcomes the final total number of deaths, the height of the peak of ICU occupancy (expressed as a fraction of the maximum bed capacity), and the corresponding peak date as $\overline{a_0}$ and $\sigma^2_{a_0}$ vary (fixing all other parameters and at $\sigma^2_{b_0} = 0$). Fig. 7 shows the resulting heatmaps for the Growth function used to model the dependency between the midpoint and the perceived severity groups (the heatmaps obtained with the other functions are shown in the Supplementary Material).

At fixed average $\overline{a_0}$, taking into account the fact that groups with different perceived severity have different behavioral parameters by increasing $\sigma^2_{a_0}$ leads to two competing effects. On the one hand, groups of individuals with high perceived severity (comprising a large fraction of the elderly population) have a higher midpoint, and thus a logistic curve describing their rate of transition to non-compliant behavior that is shifted as seen in Fig. 3: as time evolves and the vaccination campaign is rolled out, this transition rate increases only when the population vaccination rate becomes rather high. Therefore, this population relaxes its behavior later with respect to the case of $\sigma^2_{a_0} = 0$, remaining compliant with fewer contacts during a longer period. This effect would lead to a smaller impact of the epidemic as $\sigma^2_{a_0}$ increases. On the other hand, in a symmetric fashion, groups with low perceived severity have a decreasing midpoint as $\sigma^2_{a_0}$ increases, and their transition rate to non-compliance increases earlier when the vaccination is rolled out, with respect to the case of $\sigma^2_{a_0} = 0$ (see Fig. 3). The behavioral relaxation of these groups will then occur earlier, and the resulting increase in contacts will help the spread of the disease. This tends to increase the impact of the spread as $\sigma^2_{a_0}$ increases.

Let us examine the result of the interplay of these two competing effects for various values of the average $\overline{a_0}$. Let us first consider small

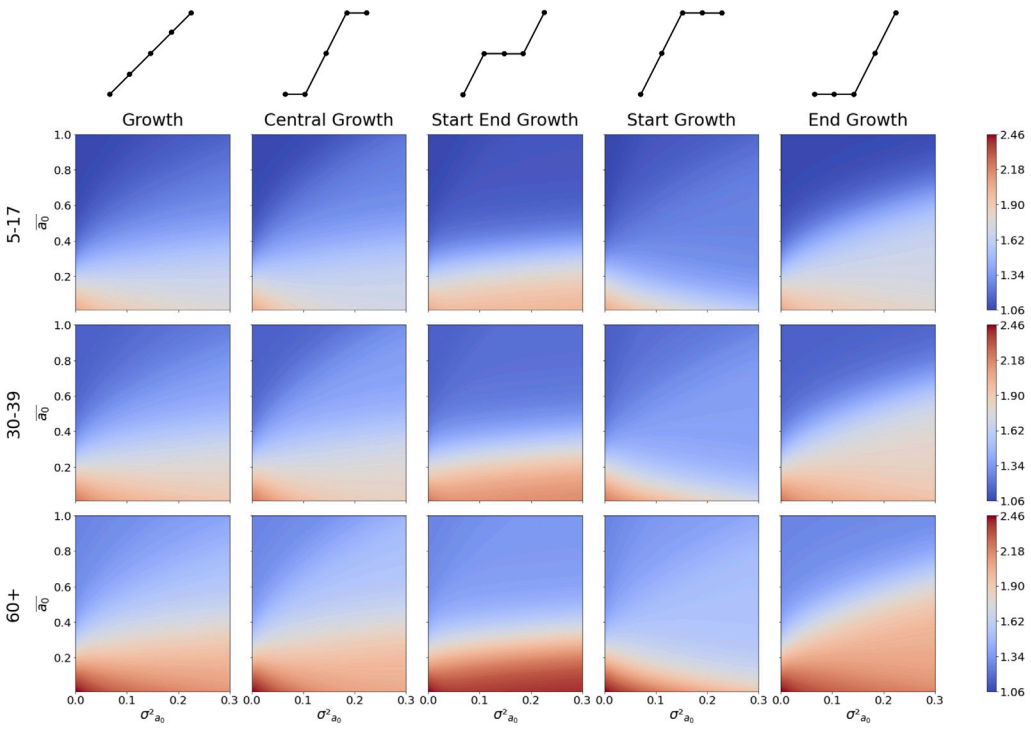

Fig. 6. Heatmaps showing the value of R_0 for three age groups (5–17, 30–39, and 60+) as a function of $\overline{a_0}$ and $\sigma^2_{a_0}$. Each heatmap refers to one age group (rows) and one of the 5 functions considered (columns). Above each column is a small diagram of the function, showing how the midpoint a_0 varies from small to high perceived severity groups (left to right). The other parameters used for the simulations are $\alpha = 10$, $\gamma = 5$, $\overline{b_0} = 0.75$, $\sigma^2_{b_0} = 0$. We employed a 900-value grid, with 30 values of $\overline{a_0}$ ranging from 0 to 1, and 30 values of $\sigma^2_{a_0}$ ranging from 0 to 0.3.

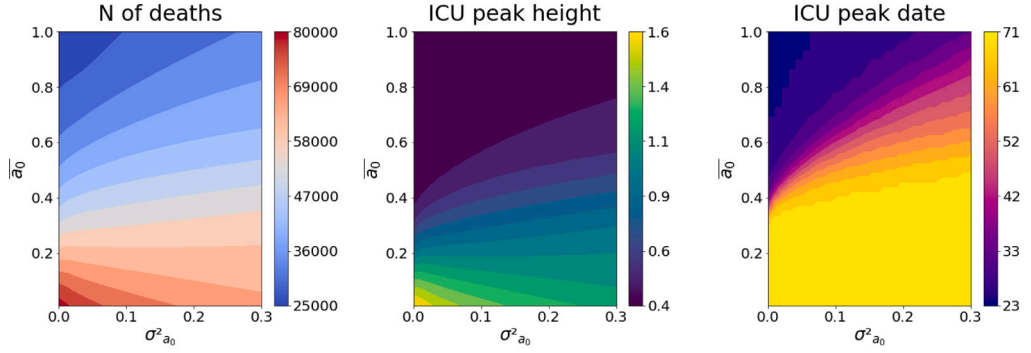

Fig. 7. Heatmaps showing the number of deaths (left), the height of the ICU peak (expressed as a fraction of the maximum bed capacity - center) and its date (expressed in days after the start of the simulation - right) as a function of $\overline{a_0}$ and $\sigma^2_{a_0}$. We used the Growth function to link perceived severity and midpoint of the logistic curve giving the transition rate from compliant to non-compliant compartments as a function of the fraction of vaccinated individuals. The other parameters used for the simulations are $\alpha = 10$, $\gamma = 5$, $\overline{b_0} = 0.75$, $\sigma^2_{b_0} = 0$. We employed a 900-value grid, with 30 values of $\overline{a_0}$ ranging from 0 to 1, and 30 values of $\sigma^2_{a_0}$ ranging from 0 to 0.3. The rugged profile of the curves related to the peak date is due to its discrete nature, with values representing the (integer) number of days after the simulation's start in which the peak is observed.

mean values of this average midpoint ($\overline{a_0} < 0.2$): this corresponds to a population that is on average poorly compliant, as the transition rates to non-compliant behavior increase rapidly when the vaccination progresses. In this case, the first effect is predominant. Indeed, increasing the variance, we observe a reduction in the number of deaths and the height of ICU peak, while the peak date remains stable at around 70 days. In particular, the strongest decrease is observed when $\overline{a_0} \approx 0$, leading approximately to a reduction in deaths over 15% and an almost 25% decrease in the ICU peak in the range of $\sigma^2_{a_0}$ explored. As $\overline{a_0}$ increases, the amplitude of the reduction decreases, and as $\overline{a_0}$ reaches ≈ 0.2, the number of deaths and the height of the ICU peak do not change when $\sigma^2_{a_0}$ increases.

For high mean values of the midpoint ($\overline{a_0} > 0.4$) instead, the population is on average largely compliant at the start of the simulation, and the transition rate to the non-compliant behavior increases only when the population is largely vaccinated. The impact of the spread is thus a decreasing function of this average at a given variance. In such cases, increasing $\sigma^2_{a_0}$ means that the groups with small perceived severity start relaxing their behavior earlier in the vaccination campaign, triggering more contacts and favoring the spread. Overall, the second effect described above prevails: even if groups with high perceived severity keep a compliant behavior longer than for $\sigma^2_{a_0} = 0$, this has little impact. Increasing $\sigma^2_{a_0}$ from 0 to 0.3 leads to an increase in the number of deaths of approximately 20% if $\overline{a_0} = 0.4$, and even of more than 30% for $\overline{a_0} > 0.75$. The maximum increase in the ICU peak height obtained when increasing $\sigma^2_{a_0}$ is reached for $\overline{a_0} = 0.4$, and smaller increases are obtained at higher mean values of the midpoint. At large $\overline{a_0}$ moreover, the peak date is sensibly delayed, at a number of days from the beginning of the simulation that can more than double. For instance when $\overline{a_0} = 0.8$ the ICU peak height changes by less than 10%

if we increase $\sigma^2_{a_0}$ from 0 to 0.3, while the peak date increases from 23 days from the start of the simulation to 47 days.

Sensitivity analysis with respect to the function used. While Fig. 7 displays the results obtained when considering the "Growth" function to link perceived severity and midpoint of the logistic curve, we have made clear when introducing the model that this function, for lack of data, is still an arbitrary modeling choice. We thus consider in the Supplementary Material the results obtained for the other functions proposed, which cover a wide range of possible functional shapes, and we compare qualitatively and quantitatively the results obtained for these various functions. Overall, the differences in the results are very small, with some small specific discrepancies. In particular, for small values of the midpoint ($\overline{a_0} < 0.2$), the later relaxation of high perceived severity groups leads to a clear reduction in deaths and ICU occupancy in all cases except for the Start End Growth Function. Indeed, in this case, by increasing $\sigma^2_{a_0}$, after a small decrease in the number of deaths, the number of severe outcomes increases, leading to a worse outcome. Among the other functions, the Start Growth function shows the strongest decrease with a 25% reduction in deaths and nearly a 40% decrease in the ICU peak when the variance increases from 0 to 0.3. Conversely, for high midpoint values ($\overline{a_0} > 0.4$), the early relaxation of low perceived severity groups compensates the benefits of the late relaxation of the groups with high perceived severity, with increasing numbers of deaths and ICU occupancy for all functions. The Start End Growth function shows a smaller increase in the number of deaths when the variance increases, while the End Growth function has the highest increase in numbers of deaths and ICU occupancy. To go beyond this qualitative comparison, we propose in the Supplementary Material a quantification of the differences between the heatmaps obtained when varying $\overline{a_0}$ and $\sigma^2_{a_0}$, obtaining small quantitative differences between the heatmaps obtained with the five different functions considered.

Sensitivity analysis with respect to the model parameters. To verify the robustness of the phenomenology described above, we perform some sensitivity analysis with respect to different parameter values (this is shown more in detail in the Supplementary Material). We explore in particular different slopes (α and γ) of the logistic functions, and a different value of the midpoint $\overline{b_0}$. In all cases, a similar picture is obtained as in Fig. 7, with only some small quantitative differences. For instance, a smaller value of $\overline{b_0}$ implies that the transition rate from non-compliant to compliant compartments increases more easily when the occupancy of ICU increases: the resulting better adoption of safe behaviors (with fewer contacts) leads thus to a decrease in the metrics describing the impact of the epidemic (number of deaths and ICU peak). Conversely, a higher $\overline{b_0}$ corresponds to a population remaining non-compliant for larger ICU occupancy values, resulting in a larger number of deaths and a higher ICU occupancy peak.

Reducing the slope α leads to logistic curves that explore a smaller range of possible values of the transition rate $\lambda_{X\to X^{NC}}$ both when the vaccination progresses and when the midpoint a_0 changes (see Fig. 2). As a result, increasing the variance $\sigma^2_{a_0}$ has a small effect on the considered metrics. On the contrary, a larger α leads to a more abrupt logistic curve and therefore to a more brutal change of $\lambda_{X\to X^{NC}}$ when the fraction of vaccinated individuals reaches the midpoint (see Fig. 2). Differences in the midpoint of different groups have then a stronger impact and the metrics investigated vary more strongly with the variance.

Changing the slope γ at fixed $\overline{b_0}$ and $\sigma^2_{b_0}$ also has a small quantitative effect: small values of γ means that the rate of transition $\lambda_{X^{NC}\to X}$ towards compliant behavior is high even for low ICU occupancy, leading thus to an overall more compliant population, a smaller number of deaths and a lower ICU peak. Conversely, a large γ with an abrupt logistic curve implies a low $\lambda_{X^{NC}\to X}$ when the ICU occupancy is below b_0, with therefore lower compliance at the beginning of the spread, and finally a stronger impact of the spread.

Finally, we present in the Supplementary Material an analysis of the impact of heterogeneity of the midpoint b_0 of the transition from non-compliant to compliant behavior (i.e., of the impact of having $\sigma^2_{b_0} > 0$). We investigate the same three metrics of the number of deaths, the ICU peak height, and the ICU peak date as a function of $\overline{b_0}$ and $\sigma^2_{b_0}$, and for 5 possible functions relating perceived severity to the midpoint value. Notably, the results for the five functions are very similar. In almost every scenario indeed, increasing the variance $\sigma^2_{b_0}$ at fixed $\overline{b_0}$ leads to an increase in the number of deaths and a later but higher peak of ICU occupancy. Indeed, the heterogeneities in the transition rate $\lambda_{X^{NC}\to X}$ mean that groups with low perceived severity go back to being compliant only for higher ICU occupancy rates, with respect to the case of $\sigma^2_{b_0} = 0$, and therefore have more contacts at the beginning of the spread, helping the disease propagate. The fact that groups with high perceived severity, on the opposite, become more compliant, is not enough to compensate for this effect.

3.4. Dynamics of the spread

Fig. 8 shows the temporal evolution of several important metrics characterizing the unfolding of the spread in the population, for a fixed average midpoint $\overline{a_0} = 0.6$, several values of the variances $\sigma^2_{a_0}$, and for a linear functional form linking perceived severity and midpoint a_0: the fraction of vaccinated individuals, of individuals in the I compartment, the cumulative fraction of cases (given by the sum of recovered individuals and deaths), of deaths and the ICU occupancy.

For $\sigma^2_{a_0} = 0$ (first column), the whole population has the same rate of relaxation to the non-compliant behavior $\lambda_{X\to X^{NC}}$. We note that the curves for the different perceived severity curves are however distinct, because of the differences in age distribution in the different groups, and of the differences in numbers of contacts and in epidemiological parameters in the different age groups. In the case considered in Fig. 8, the common midpoint $\overline{a_0}$ is rather large (60% of the population vaccinated). Thus, the rate of relaxation remains small for a long time and the population keeps a low number of contacts during the whole duration of the first peak of the epidemic curve. As the vaccination campaign progresses however, individuals start to have more contacts, and this triggers a second wave of infections, clearly seen as a second peak in the curves showing the evolution of the fraction of infected individuals. Interestingly however, as a large fraction of the population is then vaccinated, especially among the elderly given the vaccination strategy, this second peak has only a limited impact in terms of ICU occupancy and deaths.

For larger values of the variance, high perceived severity groups have a higher midpoint of the logistic curve; they thus remain compliant longer (until the vaccination reaches a larger fraction of the population). Low perceived severity groups instead have a lower midpoint and tend to relax their behavior sooner. As a result, the first peak of the fraction of infected individuals becomes higher, especially for the groups with low perceived severity (note that the final fraction of vaccinated individuals in groups of perceived severity 1 and 2 slightly decreases, because a larger fraction becomes infected and thus does not need vaccination). The second peak instead disappears. Overall, the early relaxation of behaviors of the groups with low perceived severity has an impact on the whole population: even the epidemic curves for the groups with high perceived severity change shape, with a higher early peak of cases and the disappearance of the second peak. The final total number of cases is larger for the low perceived severity groups (who, having a higher number of contacts, are particularly affected) and smaller for the high perceived severity groups (thanks to the disappearance of the second wave). However, as the early peak is higher and broader even for high perceived severity groups (largely comprised of elderly individuals), it impacts these groups at a time in which vaccine coverage is still limited and causes, therefore, a higher ICU peak and a higher number of deaths. Overall, the early relaxation even for only some groups of individuals leads to a worse outcome for

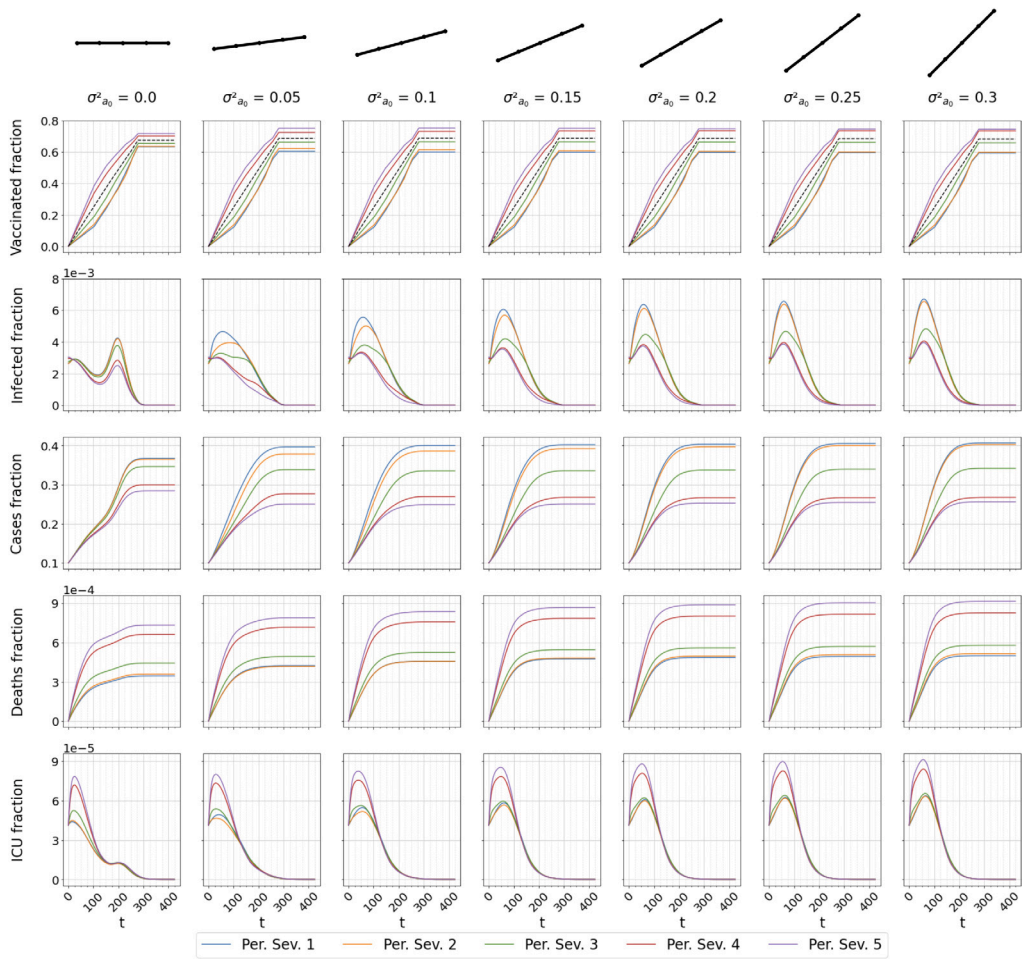

Fig. 8. Fraction of vaccinated individuals (first row - the black dashed line reports the global fraction of vaccinated individuals in the population), infected individuals (second row), cases (third row - obtained as the sum of recovered individuals and deaths), deaths (fourth row), and individuals in ICU (fifth row) as a function of time (days), for each perceived severity group. Each column corresponds to a different value of the variance $\sigma^2_{a_0}$, going from 0 to 0.3, with $\overline{a_0} = 0.6$. The other parameters are $\alpha = 10$, $\gamma = 5$, $\overline{b_0} = 0.75$, and $\sigma^2_{b_0} = 0$.

all groups of perceived severity, including the ones who remain more compliant. This result confirms indeed from a dynamical perspective the results of Fig. 7 highlighting a worsening of the final situation at high $\overline{a_0}$ when $\sigma^2_{a_0}$ increases.

Sensitivity analysis. At smaller values of the average midpoint, such as $\overline{a_0} = 0.15$, Fig. 7 showed that the increase of the variance resulted in a smaller number of deaths and ICU peak heights while maintaining peak timing. We show the impact on the epidemic dynamics of a non-zero variance for $\overline{a_0} = 0.15$ in the Supplementary Material. In scenarios without group heterogeneities ($\sigma^2_{a_0} = 0$), simultaneous behavioral relaxation occurs early, preventing second infection peaks. With higher variance ($\sigma^2_{a_0}$), infection peaks for low perceived severity groups grow taller, as their midpoint is negative, rendering them non-compliant from the start. Conversely, higher midpoints for high perceived severity groups lead to smaller infection peaks and reduced ICU occupancy. Consequently, in such scenarios, high heterogeneities in behaviors provide increased protection to high perceived severity groups, composed of a high fraction of elderly individuals, reducing, thus, severe outcomes.

We moreover check (shown in the Supplementary Material) that the shift from an epidemic curve with two peaks to one with a single peak as the variance is increased occurs for all the five functions between perceived severity and midpoint considered in the model. The evolution of the ICU curve shapes with the variance $\sigma^2_{a_0}$ is also the same for all functions investigated.

We also explore (shown in the Supplementary Material) different values of the slopes α and γ and of the midpoint $\overline{b_0}$. The shift from a two peaks profile to a single peak of the curve showing the fraction of infected individuals vs. time is obtained in almost every scenario analyzed, with the only exception of a very smooth C to NC transition (low α) or small values of $\overline{a_0}$.

We moreover investigate the impact of taking into account heterogeneities of perceived severity in the midpoints b_0 of transition rate $\lambda_{X^{NC}\to X}$, at fixed $\overline{a_0}$ and $\sigma^2_{a_0} = 0$. As $\sigma^2_{b_0}$ increases, we observe a very similar scenario as the one seen in Fig. 8: the increase in behavior heterogeneity leads to a higher first peak and to the disappearance of the second peak of the epidemic curve, with an overall increased pressure on the ICU occupancy and an increase in the number of deaths.

Finally, we perform a sensitivity analysis with respect to several epidemiological parameters (shown in the Supplementary Material), focusing in particular on vaccine efficacy, initial conditions, average length of the stay in ICU, and maximum number of ICU beds. We also consider a scenario with different latent and pre-symptomatic periods corresponding to the Alpha variant. We obtain similar results to the ones described above.

3.5. Auditing data-driven assumptions

As described in the presentation of the model, our model relies on two types of data and on one crucial mechanism that couples the evolution of the disease with the behavior of individuals in a way dependent from their disease perception. The resulting model is thus complex and relies on the availability of such data. Beyond the

Table 2
Characteristics and results for the simplified models considered.

Model	Data and assumptions	Results
Homogeneous mixing		
	Distribution in age groups.	Deaths $\geq$ 200,000 ICU $\geq 5 \cdot ICU_{max}$
Homogeneous mixing and behaviors		
	Distribution in age groups; Two classes of behaviors; Feedback loop between spreading and behaviors.	Deaths $\geq$ 120,000 for some $\overline{a_0}$ ICU $\geq 2 \cdot ICU_{max}$ for some $\overline{a_0}$ Double peak in the infection curve
Contact matrix		
	Distribution in age groups; Age-stratified contact matrix.	Deaths $<$ 100,000 ICU $< 2 \cdot ICU_{max}$ Single peak in the infection curve
Contact matrix and behaviors		
	Distribution in age groups; Age-stratified contact matrix; Two classes of behaviors; Feedback loop between spreading and behaviors.	Similar results w.r.t. the case $\sigma^2_{a_0} = 0$ of the full model; Double peak in the infection curve
Uniform distribution of perceived severity		
	Distribution in age groups; Uniform distribution in perceived severity groups Age- and perceived severity-stratified contact matrix; Two classes of behaviors; Feedback loop between spreading and behaviors.	Similar results w.r.t. full model
Same distribution of perceived severity in age groups		
	Distribution in age groups; Same distribution of perceived severity for each age group; Age- and perceived severity-stratified contact matrix; Two classes of behaviors; Feedback loop between spreading and behaviors.	Similar results w.r.t. full model
90% of population in Group 1 of perceived severity		
	Distribution in age groups; 90% of the population with perceived severity 1; Age- and perceived severity-stratified contact matrix; Two classes of behaviors; Feedback loop between spreading and behaviors.	Very small impact of varying $\sigma^2_{a_0} > 0$

sensitivity analysis with respect to parameter choices performed above, it is important to understand which data and which building blocks of the model play the most prominent role in the phenomenology we have illustrated in the previous sections. We thus consider here several models in which we remove some data sources or model mechanisms and compare the outcomes with the ones illustrated in the previous sections. We summarize the main properties and results of these models in Table 2.

Homogeneous mixing hypothesis. At the simplest level, we can hypothesize that we do not have access to the survey data, but only to census data allowing us to stratify the population in age groups, in order to retain the age-dependency of the disease parameters (such as, e.g., the IFR, which is known to depend strongly on age). We then cannot define age-stratified contact matrices and have to rely on a homogeneous mixing hypothesis.

In such a model, for the values of R_0 considered here and without the behavioral component, the number of individuals in ICU increases rapidly to over five times the maximum number of available beds, and the number of deaths more than double compared to the full model, reaching thus unrealistic numbers (see Supplementary Material for more details). Introducing the division of the population into compliant and non-compliant individuals, and incorporating the interplay between behaviors, disease spread, and vaccination, results in a decrease in deaths and ICU occupancy. However, the outcomes remain unrealistic, particularly for small values of the midpoint, where the number of deaths exceeds 120,000, and ICU occupancy rises to more than twice the maximum number of beds. Regarding the epidemiological curves, the double peak of infections due to the relaxation of behaviors can be observed for high mean values of the midpoint, similarly to the full model.

Contact matrix. As the importance of using an age-stratified contact matrix in compartmental models is well documented in literature [72–74], we next hypothesize that such data is indeed available from a survey describing contact patterns of individuals. We however assume that no data on perceived severity has been collected and do not consider any mechanisms of behavioral change. We thus obtain a model similar to the one outlined in Fig. 1 and contacts between individuals determined by their respective age and the contact matrix data, but without the non-compliant compartments and the feedback loop between behavior and spread or vaccination. By adjusting the parameter β to keep similar values of R_0 as in the full model, the peak of the ICU curve and the number of deaths remain at levels more realistic than under the homogeneous mixing hypothesis, but strongly increase (with a very high and narrow epidemic peak) as soon as R_0 increases above $\gtrapprox 2$.

Contact matrices and behaviors. Moreover, if two contact matrices are available and can be associated to compliant and non-compliant behaviors, as we have done in our model, we can add to the previous model the feedback mechanisms between the evolution of the ICU occupancy and of the vaccination campaign and the behavior and inform it using these two contact matrices: when the ICU occupancy grows, individuals tend to return to the compliant compartments, reducing their contacts and thus the spread of the virus while, when the fraction of vaccinated increases, the rate of transition to non-compliant compartments increase. The overall result of this mechanism is to produce a double peak in the epidemic curve if the parameter a_0 is large enough (see Supplementary Material), where the second peak is produced by the overall relaxation of behavior at large fractions of vaccinated, and does not lead to a large number of deaths. In fact, such a model is equivalent to the one considered in our main analysis, but with $\sigma^2_{a_0} = 0$: the parameters dictating the behavior changes are the same for the whole population, which does not allow us to investigate the impact of heterogeneities in the perception of the disease within the population.

Heterogeneity in perceived severity. The full model we have presented leverages two types of data collected in the same surveys (CoMix),

describing contacts between individuals of different age classes and giving the perceived severity of the same individuals. This allowed us to stratify the population according to both age and perceived severity. In particular, the distributions of perceived severity are different in the various age classes. We could however encounter a situation in which data on perceived severity has been collected without information on the age of the participants, or in which the data is obsolete and not necessarily fully reliable. We thus assess the robustness of our results with respect to such potential incompleteness or inaccuracy of the data on perceived severity by using different distributions of perceived severity. In a first case, we assume that the distribution of perceived severity still comes from surveys but is the same across all age groups. The second case we consider is the one of a uniform distribution of the population in the five perceived severity classes (20% of the population in each group of perceived severity). In both cases, we show in the Supplementary Material that the results are then very similar to the ones obtained when using the full information on the perceived severity distributions in the various age classes, which shows that access to this level of detail might not be required for the realism of the model. However, we also consider for completeness an unrealistic distribution in which the large majority of the population has the same perceived severity. The model's dynamics and outcomes are then driven by the behavior of this group when the variance increases, and the rich phenomenology described in the previous section is not recovered, as it stems as discussed from the competition of two effects, concerning the individuals with respectively low and large perceived severity.

Overall therefore, the construction and outcomes of our model do not crucially depend on precise and accurate information on the distributions of perceived severity in the population. However, the ability to obtain realistic values for the relevant metrics and to discuss the contrasting effects of the heterogeneity of individuals in their perceived severity depends on using realistic contact patterns and implementing a feedback loop between disease perception and behavior.

4. Discussion

The disease perception of individuals influences their adoption or disregard of preventive measures, which in turn impacts disease spread. The significance of such mechanisms is particularly pronounced during non-emergency times, such as a post-pandemic period, when the implementation of protective measures is solely reliant on individual choices and there are no top-down restrictions. Our study proposes a modeling framework that integrates disease perception, as measured by the perceived severity, as a key determinant of behavioral change. Our approach combines data sources on contact patterns and disease perception with motivated data-driven assumptions on the interplay between disease perception and behavior. Within this framework, we explored a scenario with a competition between a COVID-19 wave and a vaccination campaign, where individuals possess differences in behaviors based on their perceived severity. Individuals with low perceived severity relax behaviors sooner as the vaccination campaign progresses and adopt protective measures only when the epidemiological conditions are more severe (namely, higher occupation of ICU) than individuals with high perceived severity. We leveraged CoMix data for Italy [7,33] to inform this interplay between COVID-19 dynamics, vaccination efforts, and behavioral changes driven by perceived severity: these data make it possible on the one hand to stratify the population both in age groups and in groups of perceived severity, and on the other hand to build contact matrices describing the contacts between different groups, in both situations of compliance and non-compliance to protective measures. We moreover assumed that behavioral changes are driven on the one hand by the unfolding of the spread, as quantified by the occupancy of intensive care units, and on the other hand by the evolution of the vaccination campaign. We thus assumed that the corresponding parameters for these two processes depend on the disease perception of individuals. Our work marks a twofold addition to the current literature, putting forward a way to incorporate data sources describing disease perception into theoretical frameworks, and investigating how behavioral variations linked to perceived severity may affect disease transmission and models' dynamics and outcomes.

Results show that behavioral heterogeneities influenced by perceived severity have a substantial impact on the evolution and outcome of the epidemic. These heterogeneities generate two opposing effects. On the one hand, the longer adoption of protective measures by high perceived severity groups (comprising a high proportion of elderly individuals) resulted in higher protection for those individuals. On the other hand, virus spread was facilitated by low perceived severity groups relaxing behaviors more easily. The prevailing effect depended on the overall behavior of the population. In populations that were overall less compliant on average, characterized by high numbers of deaths and ICU peaks, increasing behavioral heterogeneities led to a reduction in these metrics. Conversely, in populations that were on average more compliant, lower severe outcomes were observed, but increasing heterogeneities resulted in an increase in deaths and ICU occupancy. Epidemiological curves gave more insight into this phenomenology. Indeed, when differences in behaviors among groups were not taken into account, we observed a double peak in the evolution of the fraction of infected: the second peak was due to the contemporary relaxation of behaviors by the whole population when the vaccination campaign reached a large enough fraction of the population. Thanks to the high immunization provided by the vaccine, this second peak had small consequences in terms of ICU occupancy and deaths. On the contrary, an increase in the heterogeneities among perceived severity groups caused the disappearance of the second infection peak in favor of a higher first peak for the whole population, resulting in more deaths and ICU hospitalizations, due to the absence of widespread vaccine protection at the time of this first peak. Additionally, our simulations revealed that the specific way we modeled the dependency between behavior relaxation and perceived severity had a small impact on crucial metrics such as the number of deaths and the height of the ICU peak. The sensitivity analysis reported in the Supplementary Material confirmed the robustness of our results. Modifying key epidemiological parameters provided similar pictures, with behavioral heterogeneities consistently impacting metrics and epidemic peaks in the same way across the majority of analyzed scenarios. As our modeling framework relies on the one hand on specific data describing both contact patterns and distribution of perceived severity in the various age groups forming the population, and on the other hand on a feedback mechanism between spread and behavior, we have moreover considered several models relying on less data or where the feedback is not taken into account. Interestingly, we obtained a phenomenology similar to the model informed with the full data as long as (i) the model takes into account the age-stratified contact patterns of the population, (ii) the feedback mechanism was included and (iii) the population was distributed in groups with different perceived severity, even if the corresponding information was not fully precise or accurate.

Our study comes with several limitations worth discussing. First, the age- and perceived severity-stratified contact matrix we build are based not only on survey data but also on the assumption that contacts between individuals in different perceived-severity groups within an age group are proportional to their respective sizes. This assumption neglects possible correlations in contact patterns such as potential homophily effects between individuals with low perceived severity and low compliance to health recommendations [75]. Even if this assumption might not capture the full complexity of real-world contact patterns, including homophily effects without relevant data would lead to the introduction of additional parameters, and we leave the investigation of such effects to future work. We have also assumed that the perceived severity of individuals is constant, while it may vary over the course of the spread. Data indicate however that the corresponding variations are limited, and moreover we have seen that the model is robust with respect to changes in the distribution of the population

in perceived severity groups. Moreover, even if the amount of data in our framework remains limited, while they still play a relevant role in shaping the specific assumptions at the core of the model, we rely on assumptions for which no quantitative empirical validation is available at this stage. In particular, while the choice of logistic functions to rely the rates of behavior change with their drivers (vaccination rate or ICU occupancy) can be justified in relation with studies on behavior adoption [41–43], the parameters of these logistics and their dependence on perceived severity are not derived from empirical data. We have however considered five different choices of such functional dependence and shown the robustness of the phenomenology with respect to this arbitrary choice. Furthermore, we considered a very simple vaccination mechanism. We included in the model a single dose instead of two or more, we assumed a fully working vaccine from the beginning, with no waning phenomenon. We finally note that the theoretical framework we have presented and explored is intended not for making specific predictions on disease spreading, but rather for conducting comparative analyses of hypothetical scenarios.

Our work has on the other hand some important research and public health implications. Our modeling framework is a step towards a more comprehensive understanding of how disease perception, particularly perceived severity, can impact the complex dynamics of disease spreading, and of how data on disease perception might be included into models. The strong impact of differences in disease perception on the model's outcome highlights the importance of taking such heterogeneities into account in models aiming to capture the dynamics of infectious disease transmission and calls for more extensive, continuative, and comprehensive data collections to help uncover which aspects of behavior are most influential. In particular, this study adds insights to the relatively limited empirical research in this area, setting the stage for further exploration and broader understanding necessary to better grasp human adaptive behaviors, especially during non-emergency times. Interestingly, we have found that the lack of very precise information on the distribution of perceived severity in the population is not a crucial prerequisite for this kind of modeling. This indicates that even survey efforts that are limited to interaction patterns and do not tackle disease perceptions can still be used to inform models including feedback mechanisms between perception and behavior. On the other hand, our use of several assumptions, which is dictated by the lack of corresponding empirical insights, also shows that further targeted data collection work is needed. In particular, the insights gained pave the way for creating additional data collections drawing on individuals' personal experiences and perceived risks and their temporal evolution, to help study individual and collective protective strategies. Importantly, there is a need for both large-scale and small-scale data collection efforts (including in-depth interviews) to obtain more detailed and nuanced information, in particular to investigate whether individuals with similar perceived severity tend to have more contacts, a pattern that would influence the contact matrix patterns and might have an impact on the epidemic's unfolding. From the perspective of public health, a data-informed identification of the principal factors that drive changes in behavior would also provide new ways for predicting these shifts and creating more effective communication strategies to reduce transmission among individuals. For instance, our model's results highlight how the relaxation of behaviors by a limited fraction of the population, who experience a low perceived severity, can negatively impact other groups of the population even if those continue to adopt a self-protective behavior. Communication strategies should thus raise awareness of the global benefits of protective behaviors especially in those groups of the population who are less likely to be affected severely by the disease, to highlight the benefits for at-risk populations.

CRediT authorship contribution statement

Alessandro De Gaetano: Writing – review & editing, Writing – original draft, Visualization, Validation, Software, Methodology, Investigation, Formal analysis, Data curation, Conceptualization. **Alain Barrat:** Writing – review & editing, Visualization, Supervision, Methodology, Investigation, Conceptualization. **Daniela Paolotti:** Writing – review & editing, Visualization, Supervision, Methodology, Investigation, Conceptualization.

Declaration of competing interest

The authors declare that they have no known competing financial interests or personal relationships that could have appeared to influence the work reported in this paper.

Acknowledgments

DP and ADG acknowledge support by the VERDI project (101045989), funded by the European Union. Views and opinions expressed in this article are however those of the author(s) only and do not necessarily reflect those of the European Union or the Health and Digital Executive Agency. Neither the European Union nor the granting authority can be held responsible for them. AB acknowledges support from the Agence Nationale de la Recherche (ANR) project DATAREDUX (ANR-19-CE46-0008). All the authors are grateful to Dr Michele Tizzani for support with CoMix data and useful discussions.

Appendix A. Supplementary data

Supplementary material related to this article can be found online at https://doi.org/10.1016/j.mbs.2024.109337.

References

[1] N. Ferguson, Capturing human behaviour, Nature 446 (7137) (2007) 733–733.
[2] A. Vespignani, Predicting the behavior of techno-social systems, Science 325 (5939) (2009) 425–428.
[3] N. Perra, D. Balcan, B. Gonçalves, A. Vespignani, Towards a characterization of behavior-disease models, PLoS One 6 (8) (2011) e23084.
[4] S. Funk, M. Salathé, V.A. Jansen, Modelling the influence of human behaviour on the spread of infectious diseases: a review, J. R. Soc. Interface 7 (50) (2010) 1247–1256.
[5] F. Verelst, L. Willem, P. Beutels, Behavioural change models for infectious disease transmission: a systematic review (2010–2015), J. R. Soc. Interface 13 (125) (2016) 20160820.
[6] N. Perra, Non-pharmaceutical interventions during the COVID-19 pandemic: A review, Phys. Rep. 913 (2021) 1–52.
[7] F. Verelst, L. Hermans, S. Vercruysse, A. Gimma, P. Coletti, J.A. Backer, K.L. Wong, J. Wambua, K. van Zandvoort, L. Willem, et al., SOCRATES-CoMix: a platform for timely and open-source contact mixing data during and in between COVID-19 surges and interventions in over 20 European countries, BMC Med. 19 (1) (2021) 1–7.
[8] J.A. Salomon, A. Reinhart, A. Bilinski, E.J. Chua, W. La Motte-Kerr, M.M. Rönn, M.B. Reitsma, K.A. Morris, S. LaRocca, T.H. Farag, et al., The US COVID-19 trends and impact survey: Continuous real-time measurement of COVID-19 symptoms, risks, protective behaviors, testing, and vaccination, Proc. Natl. Acad. Sci. 118 (51) (2021) e2111454118.
[9] Google LLC, Google COVID-19 community mobility reports, https://www.google.com/covid19/mobility/ (Accessed: 20 September 2023).
[10] T. Hale, N. Angrist, B. Kira, A. Petherick, T. Phillips, S. Webster, Variation in government responses to COVID-19, 2020, University of Oxford.
[11] E. Del Fava, J. Cimentada, D. Perrotta, A. Grow, F. Rampazzo, S. Gil-Clavel, E. Zagheni, Differential impact of physical distancing strategies on social contacts relevant for the spread of SARS-CoV-2: evidence from a cross-national online survey, March–April 2020, BMJ Open 11 (10) (2021) e050651.
[12] U. Basellini, D. Alburez-Gutierrez, E. Del Fava, D. Perrotta, M. Bonetti, C.G. Camarda, E. Zagheni, Linking excess mortality to mobility data during the first wave of COVID-19 in England and Wales, SSM-Popul. Health 14 (2021) 100799.
[13] Y. Ge, W.-B. Zhang, H. Liu, C.W. Ruktanonchai, M. Hu, X. Wu, Y. Song, N.W. Ruktanonchai, W. Yan, E. Cleary, et al., Impacts of worldwide individual non-pharmaceutical interventions on COVID-19 transmission across waves and space, Int. J. Appl. Earth Obs. Geoinf. 106 (2022) 102649.

[14] J. Vlachos, E. Hertegård, H. B. Svaleryd, The effects of school closures on SARS-CoV-2 among parents and teachers, Proc. Natl. Acad. Sci. 118 (9) (2021) e2020834118.

[15] T. Hale, N. Angrist, A.J. Hale, B. Kira, S. Majumdar, A. Petherick, T. Phillips, D. Sridhar, R.N. Thompson, S. Webster, et al., Government responses and COVID-19 deaths: Global evidence across multiple pandemic waves, PLoS One 16 (7) (2021) e0253116.

[16] M. Galanti, S. Pei, T.K. Yamana, F.J. Angulo, A. Charos, D.L. Swerdlow, J. Shaman, Social distancing remains key during vaccinations, Science 371 (6528) (2021) 473–474.

[17] N. Gozzi, P. Bajardi, N. Perra, The importance of non-pharmaceutical interventions during the COVID-19 vaccine rollout, PLoS Comput. Biol. 17 (9) (2021) e1009346.

[18] C.N. Ngonghala, A.B. Gumel, Mathematical assessment of the role of vaccination against COVID-19 in the United States, in: Mathematical Modelling, Simulations, and AI for Emergent Pandemic Diseases, Elsevier, 2023, pp. 221–249.

[19] C.N. Ngonghala, H.B. Taboe, S. Safdar, A.B. Gumel, Unraveling the dynamics of the omicron and delta variants of the 2019 coronavirus in the presence of vaccination, mask usage, and antiviral treatment, Appl. Math. Model. 114 (2023) 447–465.

[20] I.M. Rosenstock, The health belief model and preventive health behavior, Health Educ. Monographs 2 (4) (1974) 354–386.

[21] G.M. Hochbaum, Public participation in medical screening programs: A socio-psychological study, vol. 572, US Department of Health, Education, and Welfare, Public Health Service . . . , 1958.

[22] J. Hayden, Introduction To Health Behavior Theory, Jones & Bartlett Learning, 2022.

[23] H. Seale, A.E. Heywood, J. Leask, M. Sheel, S. Thomas, D.N. Durrheim, K. Bolsewicz, R. Kaur, COVID-19 is rapidly changing: Examining public perceptions and behaviors in response to this evolving pandemic, PLoS One 15 (6) (2020) e0235112.

[24] W.B. De Bruin, D. Bennett, Relationships between initial COVID-19 risk perceptions and protective health behaviors: a national survey, Am. J. Prev. Med. 59 (2) (2020) 157–167.

[25] N.T. Brewer, N.D. Weinstein, C.L. Cuite, J.E. Herrington, Risk perceptions and their relation to risk behavior, Annal. Behav. Med. 27 (2004) 125–130.

[26] N.D. Weinstein, A. Kwitel, K.D. McCaul, R.E. Magnan, M. Gerrard, F.X. Gibbons, Risk perceptions: assessment and relationship to influenza vaccination, Health Psychol. 26 (2) (2007) 146.

[27] R.A. Ferrer, W.M. Klein, Risk perceptions and health behavior, Curr. Opin. Psychol. 5 (2015) 85–89.

[28] Z. Vally, Public perceptions, anxiety and the perceived efficacy of health-protective behaviours to mitigate the spread of the SARS-Cov-2/COVID-19 pandemic, Publ. Health 187 (2020) 67–73.

[29] S. Dryhurst, C.R. Schneider, J. Kerr, A.L. Freeman, G. Recchia, A.M. Van Der Bles, D. Spiegelhalter, S. Van Der Linden, Risk perceptions of COVID-19 around the world, J. Risk Res. 23 (7–8) (2020) 994–1006.

[30] C.R. Schneider, S. Dryhurst, J. Kerr, A.L. Freeman, G. Recchia, D. Spiegelhalter, S. van der Linden, COVID-19 risk perception: a longitudinal analysis of its predictors and associations with health protective behaviours in the United Kingdom, J. Risk Res. 24 (3–4) (2021) 294–313.

[31] M. Siegrist, L. Luchsinger, A. Bearth, The impact of trust and risk perception on the acceptance of measures to reduce COVID-19 cases, Risk Anal. 41 (5) (2021) 787–800.

[32] A. Kaim, M. Siman-Tov, E. Jaffe, B. Adini, Factors that enhance or impede compliance of the public with governmental regulation of lockdown during COVID-19 in Israel, Int. J. Disas. Risk Reduct. 66 (2021) 102596.

[33] J. Wambua, N. Loedy, C.I. Jarvis, K.L.M. Wong, C. Faes, R. Grah, B. Prasse, F. Sandmann, R. Niehus, H. Johnson, W. Edmunds, P. Beutels, N. Hens, P. Coletti, The influence of COVID-19 risk perception and vaccination status on the number of social contacts across Europe: insights from the CoMix study, BMC Public Health 23 (2023) 1350.

[34] T. Harris, P. Jayasundara, R. Ragonnet, J. Trauer, N. Geard, C. Zachreson, Apparent structural changes in contact patterns during COVID-19 were driven by survey design and long-term demographic trends, 2024, arXiv preprint arXiv:2406.01639.

[35] Italian ministerial decree (DPCM) of 03/11/2020, https://www.salute.gov.it/portale/nuovocoronavirus/dettaglioNotizieNuovoCoronavirus.jsp?lingua=english&menu=notizie&p=dalministero&id=5154.

[36] United Nations, Department of Economic and Social Affairs, Population Division. World Population Prospects: The 2019 Revision; 2020, https://population.un.org/wpp/Download/Metadata/Documentation/.

[37] M. Tizzani, A. De Gaetano, C.I. Jarvis, A. Gimma, K. Wong, W.J. Edmunds, P. Beutels, N. Hens, P. Coletti, D. Paolotti, Impact of tiered measures on social contact and mixing patterns of in Italy during the second wave of COVID-19, BMC Public Health 23 (1) (2023) 906.

[38] E. Commodari, V.L. La Rosa, Adolescents in quarantine during COVID-19 pandemic in Italy: perceived health risk, beliefs, psychological experiences and expectations for the future, Front. Psychol. 11 (2020) 559951.

[39] L. Matrajt, J. Eaton, T. Leung, E.R. Brown, Vaccine optimization for COVID-19: Who to vaccinate first? Sci. Adv. 7 (6) (2021) eabf1374.

[40] L. Matrajt, J. Eaton, T. Leung, D. Dimitrov, J.T. Schiffer, D.A. Swan, H. Janes, Optimizing vaccine allocation for COVID-19 vaccines shows the potential role of single-dose vaccination, Nat. Commun. 12 (1) (2021) 3449.

[41] R. Aiyappa, A. Flammini, Y.-Y. Ahn, Emergence of simple and complex contagion dynamics from weighted belief networks, Sci. Adv. 10 (15) (2024) eadh4439.

[42] E.M. Rogers, A. Singhal, M.M. Quinlan, Diffusion of innovations, in: An Integrated Approach To Communication Theory and Research, Routledge, 2014, pp. 432–448.

[43] S.M. Reader, Distinguishing social and asocial learning using diffusion dynamics, Anim. Learn. Behav. 32 (1) (2004) 90–104.

[44] J. Wambua, L. Hermans, P. Coletti, F. Verelst, L. Willem, C.I. Jarvis, A. Gimma, K.L. Wong, A. Lajot, S. Demarest, et al., The influence of risk perceptions on close contact frequency during the SARS-CoV-2 pandemic, Sci. Rep. 12 (1) (2022) 5192.

[45] A. Gimma, J.D. Munday, K.L. Wong, P. Coletti, K. van Zandvoort, K. Prem, C.C.-. working group, P. Klepac, G.J. Rubin, S. Funk, et al., Changes in social contacts in England during the COVID-19 pandemic between March 2020 and March 2021 as measured by the CoMix survey: A repeated cross-sectional study, PLoS Med. 19 (3) (2022) e1003907.

[46] S.A. Lauer, K.H. Grantz, Q. Bi, F.K. Jones, Q. Zheng, H.R. Meredith, A.S. Azman, N.G. Reich, J. Lessler, The incubation period of coronavirus disease 2019 (COVID-19) from publicly reported confirmed cases: estimation and application, Annal. Intern. Med. 172 (9) (2020) 577–582.

[47] L. Ferretti, C. Wymant, M. Kendall, L. Zhao, A. Nurtay, L. Abeler-Dörner, M. Parker, D. Bonsall, C. Fraser, Quantifying SARS-CoV-2 transmission suggests epidemic control with digital contact tracing, Science 368 (6491) (2020) eabb6936.

[48] M. Kang, H. Xin, J. Yuan, S.T. Ali, Z. Liang, J. Zhang, T. Hu, E.H. Lau, Y. Zhang, M. Zhang, et al., Transmission dynamics and epidemiological characteristics of SARS-CoV-2 Delta variant infections in Guangdong, China, May to June 2021, Eurosurveillance 27 (10) (2022) 2100815.

[49] COVID-19 Omicron variant infectious period and transmission from people with asymptomatic compared with symptomatic infection: a rapid review, https://assets.publishing.service.gov.uk/government/uploads/system/uploads/attachment_data/file/1145484/COVID-19-infectiousness-_asymptomatic-transmission.pdf.

[50] S.M. Kissler, C. Tedijanto, E. Goldstein, Y.H. Grad, M. Lipsitch, Projecting the transmission dynamics of SARS-CoV-2 through the postpandemic period, Science 368 (6493) (2020) 860–868.

[51] F. Riccardo, M. Ajelli, X.D. Andrianou, A. Bella, M. Del Manso, M. Fabiani, S. Bellino, S. Boros, A.M. Urdiales, V. Marziano, et al., Epidemiological characteristics of COVID-19 cases and estimates of the reproductive numbers 1 month into the epidemic, Italy, 28 January to 31 March 2020, Eurosurveillance 25 (49) (2020) 2000790.

[52] R. Li, S. Pei, B. Chen, Y. Song, T. Zhang, W. Yang, J. Shaman, Substantial undocumented infection facilitates the rapid dissemination of novel coronavirus (SARS-CoV-2), Science 368 (6490) (2020) 489–493.

[53] E. Colosi, G. Bassignana, D.A. Contreras, C. Poirier, P.-Y. Boëlle, S. Cauchemez, Y. Yazdanpanah, B. Lina, A. Fontanet, A. Barrat, et al., Screening and vaccination against COVID-19 to minimise school closure: a modelling study, The Lancet Infect. Dis. 22 (7) (2022) 977–989.

[54] Y. Liu, A.A. Gayle, A. Wilder-Smith, J. Rocklöv, The reproductive number of COVID-19 is higher compared to SARS coronavirus, J. Travel Med. (2020).

[55] D. Cereda, M. Manica, M. Tirani, F. Rovida, V. Demicheli, M. Ajelli, P. Poletti, F. Trentini, G. Guzzetta, V. Marziano, et al., The early phase of the COVID-19 epidemic in Lombardy, Italy, Epidemics 37 (2021) 100528.

[56] Centers for Disease Control and Prevention: COVID-19 Pandemic Planning Scenarios, https://www.cdc.gov/coronavirus/2019-ncov/hcp/planning-scenarios.html#table-1.

[57] R. Verity, L.C. Okell, I. Dorigatti, P. Winskill, C. Whittaker, N. Imai, G. Cuomo-Dannenburg, H. Thompson, P.G. Walker, H. Fu, et al., Estimates of the severity of coronavirus disease 2019: a model-based analysis, The Lancet Infect. Dis. 20 (6) (2020) 669–677.

[58] H. Salje, C. Tran Kiem, N. Lefrancq, N. Courtejoie, P. Bosetti, J. Paireau, A. Andronico, N. Hozé, J. Richet, C.-L. Dubost, et al., Estimating the burden of SARS-CoV-2 in France, Science 369 (6500) (2020) 208–211.

[59] P.D.W. Garcia, T. Fumeaux, P. Guerci, D.M. Heuberger, J. Montomoli, F. Roche-Campo, R.A. Schuepbach, M.P. Hilty, M.A. Farias, A. Margarit, et al., Prognostic factors associated with mortality risk and disease progression in 639 critically ill patients with COVID-19 in europe: Initial report of the international RISC-19-ICU prospective observational cohort, EClinicalMedicine 25 (2020).

[60] M. Giancotti, Responses of Italian public hospitals to COVID-19 pandemic: analysis of supply and demand of hospital ICU beds, in: Med. Sci. Forum, 4, (1) MDPI, 2021, p. 16.

[61] E. Mathieu, H. Ritchie, L. Rodés-Guirao, C. Appel, C. Giattino, J. Hasell, B. Macdonald, S. Dattani, D. Beltekian, E. Ortiz-Ospina, M. Roser, Coronavirus pandemic (COVID-19), Our World in Data (2020) https://ourworldindata.org/coronavirus.

[62] C.U. Worldometer, Cases and deaths from COVID-19 virus pandemic for Italy, https://www.worldometers.info/coronavirus/country/italy.
[63] S. Paduano, P. Galante, N. Berselli, L. Ugolotti, A. Modenese, A. Poggi, M. Malavolti, S. Turchi, I. Marchesi, R. Vivoli, et al., Seroprevalence survey of anti-SARS-CoV-2 antibodies in a population of Emilia-Romagna region, Northern Italy, Int. J. Environ. Res. Public Health 19 (13) (2022) 7882.
[64] S. Marchi, C. Coppola, P. Piu, L. Benincasa, F. Dapporto, A. Manenti, S. Viviani, E. Montomoli, C.M. Trombetta, SARS-CoV-2 epidemiological trend before vaccination era: a seroprevalence study in Apulia, Southern Italy, in 2020, J. Publ. Health (2023) 1–6.
[65] W. Wang, Q. Wu, J. Yang, K. Dong, X. Chen, X. Bai, X. Chen, Z. Chen, C. Viboud, M. Ajelli, et al., Global, regional, and national estimates of target population sizes for covid-19 vaccination: descriptive study, bmj 371 (2020).
[66] K.M. Bubar, K. Reinholt, S.M. Kissler, M. Lipsitch, S. Cobey, Y.H. Grad, D.B. Larremore, Model-informed COVID-19 vaccine prioritization strategies by age and serostatus, Science 371 (6352) (2021) 916–921.
[67] J.L. Bernal, N. Andrews, C. Gower, C. Robertson, J. Stowe, E. Tessier, R. Simmons, S. Cottrell, R. Roberts, M. O'Doherty, et al., Effectiveness of the Pfizer-BioNTech and oxford-AstraZeneca vaccines on covid-19 related symptoms, hospital admissions, and mortality in older adults in England: test negative case-control study, bmj 373 (2021).
[68] K.B. Pouwels, E. Pritchard, P.C. Matthews, N. Stoesser, D.W. Eyre, K.-D. Vihta, T. House, J. Hay, J.I. Bell, J.N. Newton, et al., Effect of delta variant on viral burden and vaccine effectiveness against new SARS-CoV-2 infections in the UK, Nature Med. 27 (12) (2021) 2127–2135.
[69] C. Zheng, W. Shao, X. Chen, B. Zhang, G. Wang, W. Zhang, Real-world effectiveness of COVID-19 vaccines: a literature review and meta-analysis, Int. J. Infect. Dis. 114 (2022) 252–260.
[70] A. De Gaetano, P. Bajardi, N. Gozzi, N. Perra, D. Perrotta, D. Paolotti, Behavioral changes associated with COVID-19 vaccination: Cross-national online survey, J. Med. Internet Res. 25 (2023) e47563.
[71] A.D. Gaetano, Repository with the code for the analysis, https://github.com/aledega/perceived-severity-behaviors.
[72] H.W. Hethcote, Modeling heterogeneous mixing in infectious disease dynamics, in: MOdels for Infectious Human Diseases: Their Structure and Relation to Data, vol. 215, Cambridge University Press Cambridge, UK, 1996, p. 238.
[73] J. Mossong, N. Hens, M. Jit, P. Beutels, K. Auranen, R. Mikolajczyk, M. Massari, S. Salmaso, G.S. Tomba, J. Wallinga, et al., Social contacts and mixing patterns relevant to the spread of infectious diseases, PLoS Med. 5 (3) (2008) e74.
[74] K. Prem, A.R. Cook, M. Jit, Projecting social contact matrices in 152 countries using contact surveys and demographic data, PLoS Comput. Biol. 13 (9) (2017) e1005697.
[75] L.G. Alvarez-Zuzek, C.M. Zipfel, S. Bansal, Spatial clustering in vaccination hesitancy: The role of social influence and social selection, PLoS Comput. Biol. 18 (10) (2022) 1–19, http://dx.doi.org/10.1371/journal.pcbi.1010437.